

Computational Statistics on the Sphere

Ben Wandelt

Institut d'Astrophysique de Paris (IAP)

Lagrange Institute Paris (ILP)

UPMC

Sorbonne Université

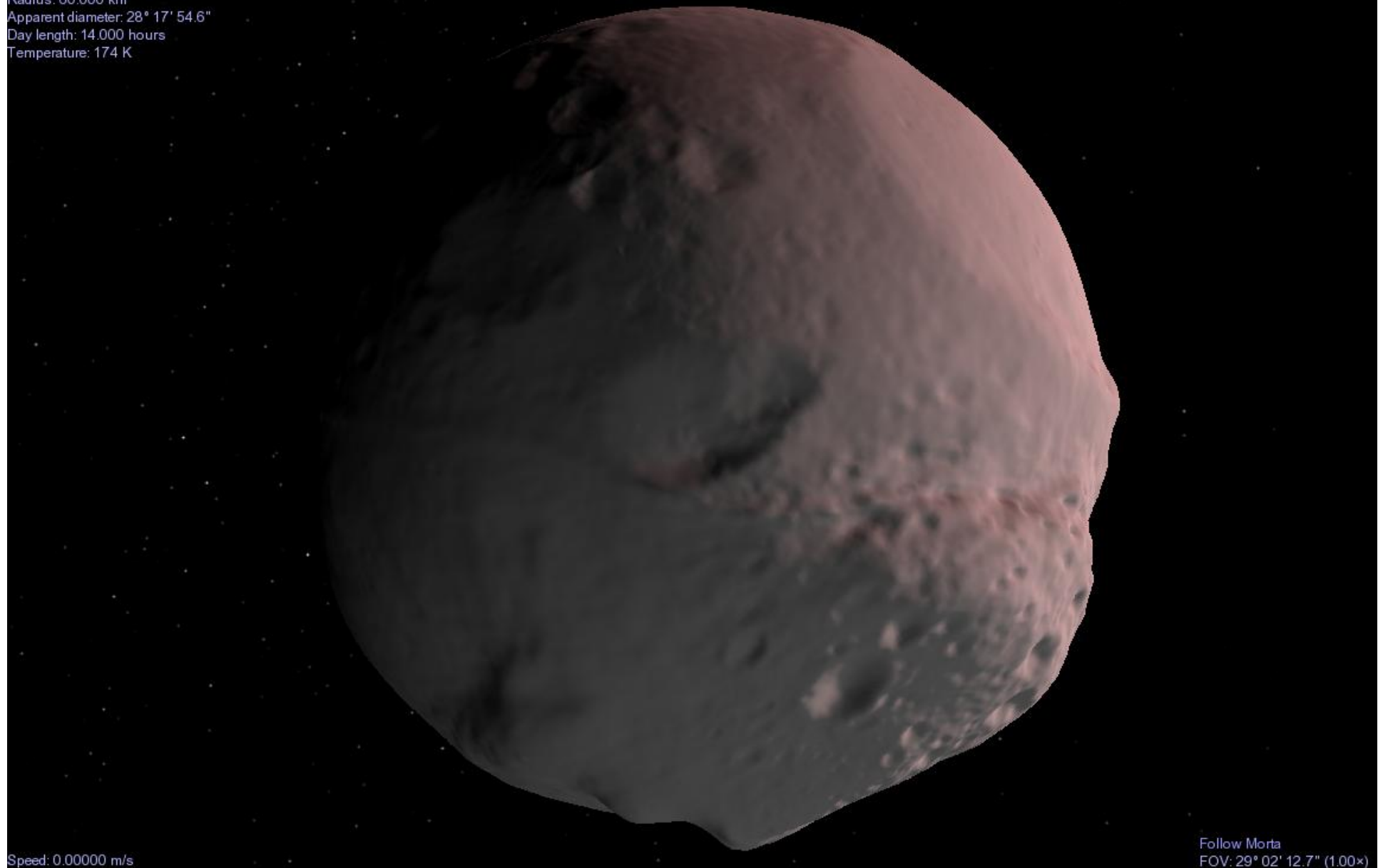


Image Credit: Chip Clark, Smithsonian Institution

Morta

Distance: 185.45 km
Radius: 60.000 km
Apparent diameter: 28° 17' 54.6"
Day length: 14.000 hours
Temperature: 174 K

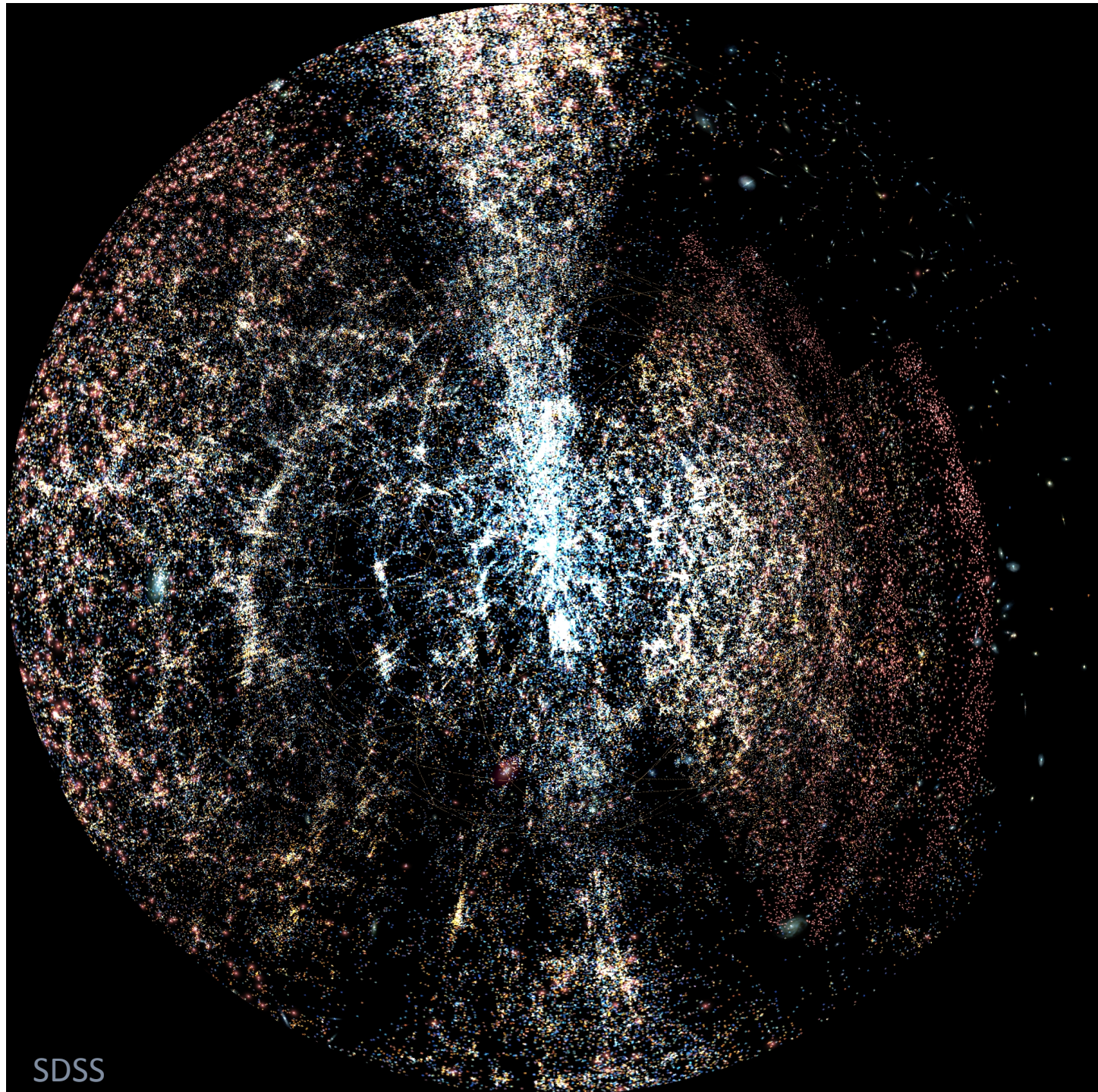
2006 08 21 17:16:14 UTC
1,000× faster (Paused)



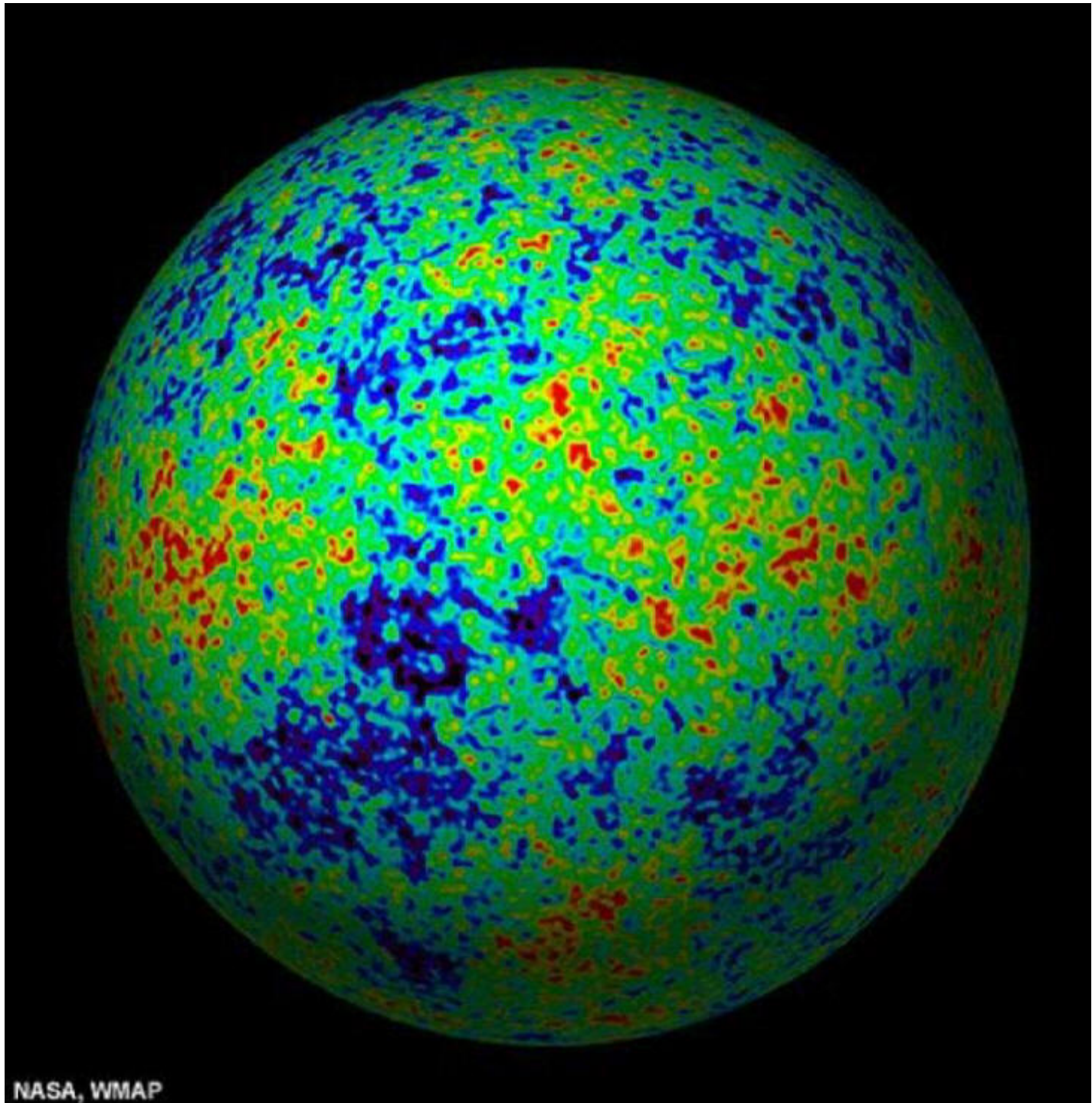
Speed: 0.00000 m/s

Follow Mirta
FOV: 29° 02' 12.7" (1.00×)

Ben Wandelt, IAP

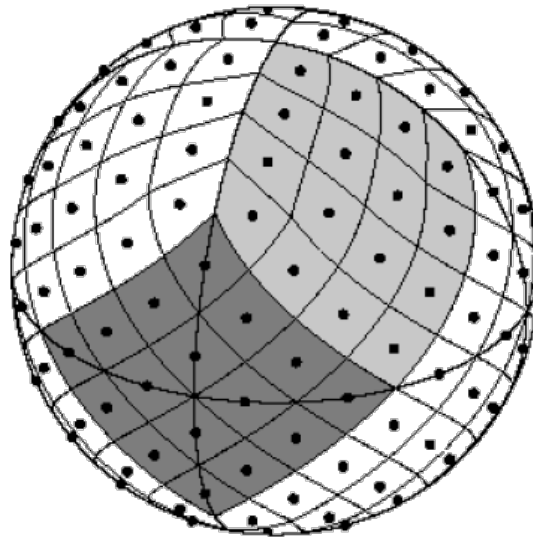


SDSS



NASA, WMAP

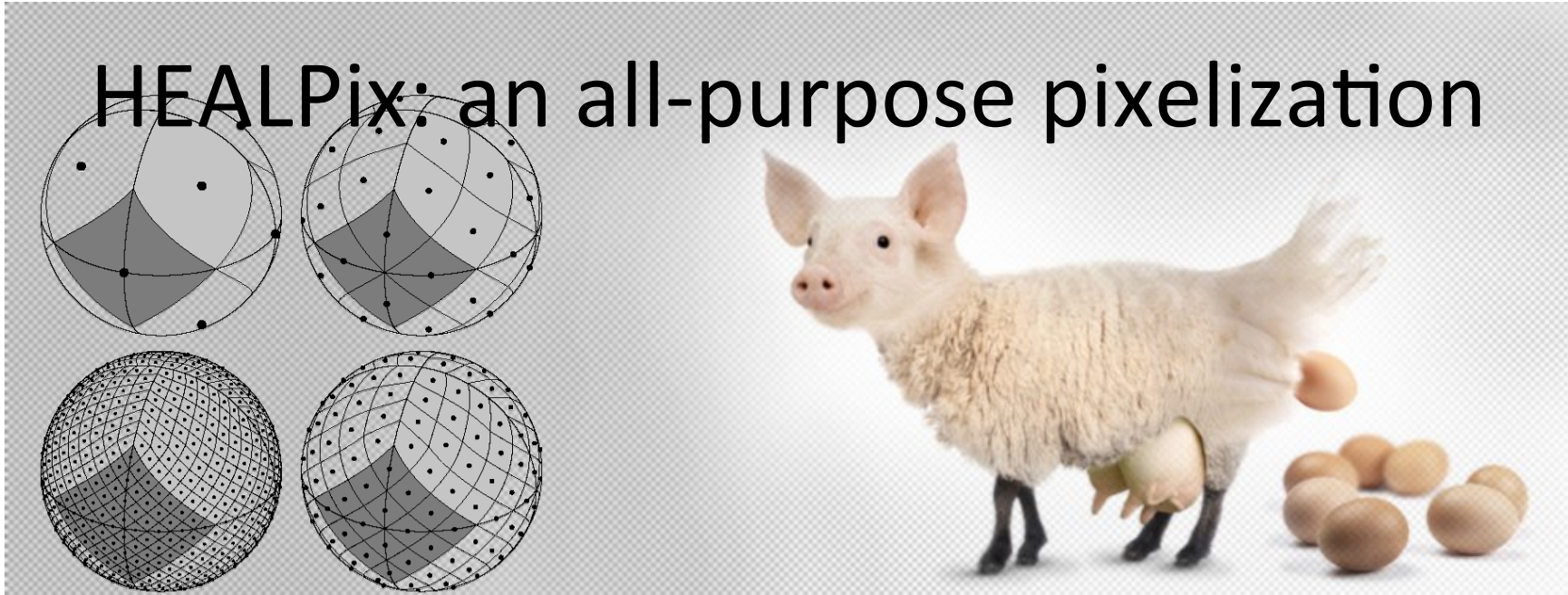
Pixelizing the sphere: HEALPix



healpix.jpl.nasa.gov

Górski, Hivon, BDW 1999; Górski et al 2005

HEALPix: an all-purpose pixelization

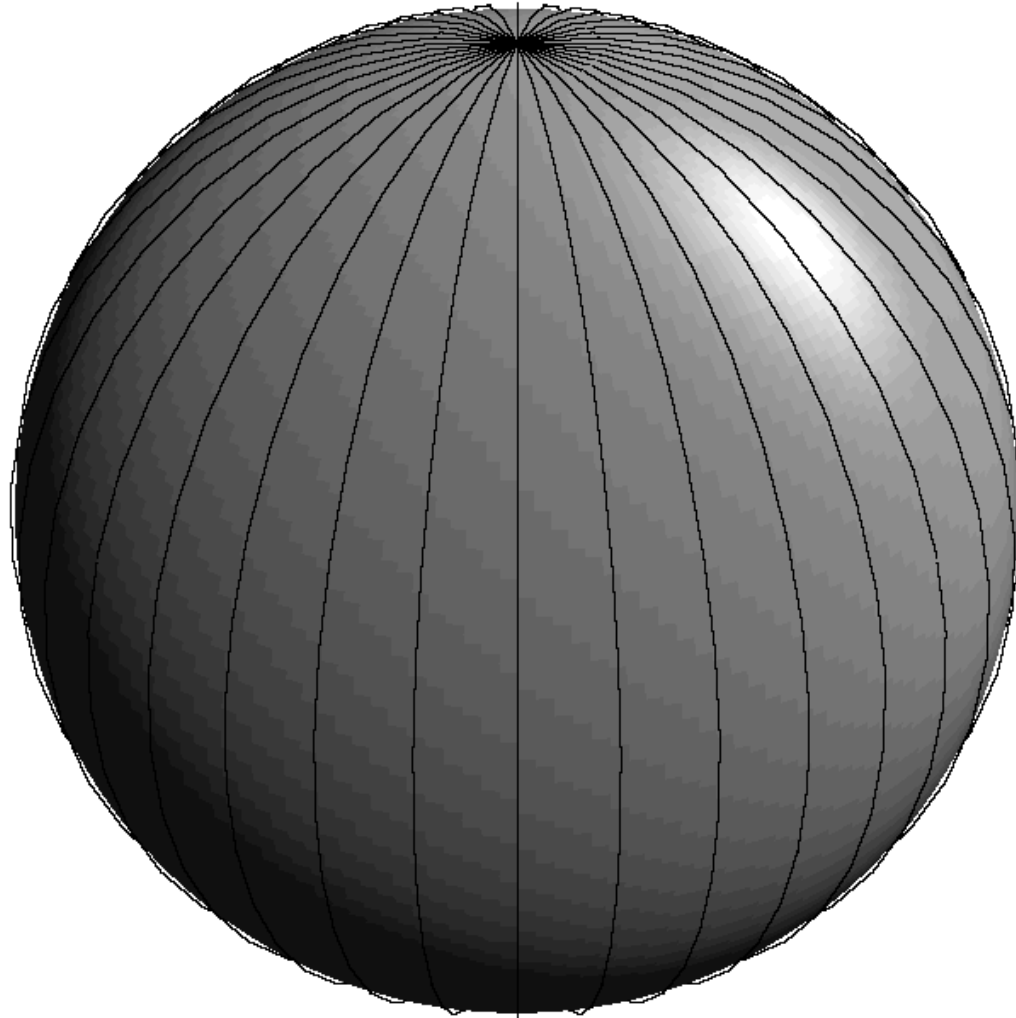


- Hierarchical grid enables adaptive refinement
- Equal Area pixels: approximately uniform coverage on the sphere, good quadrature properties
- Equal Latitude rings: fast SHTs in $O(L^3)$ ops for bandlimit L
- Symmetries: simplifies code and allows compressing distance graph between pixels
- Analytic description of pixel boundaries

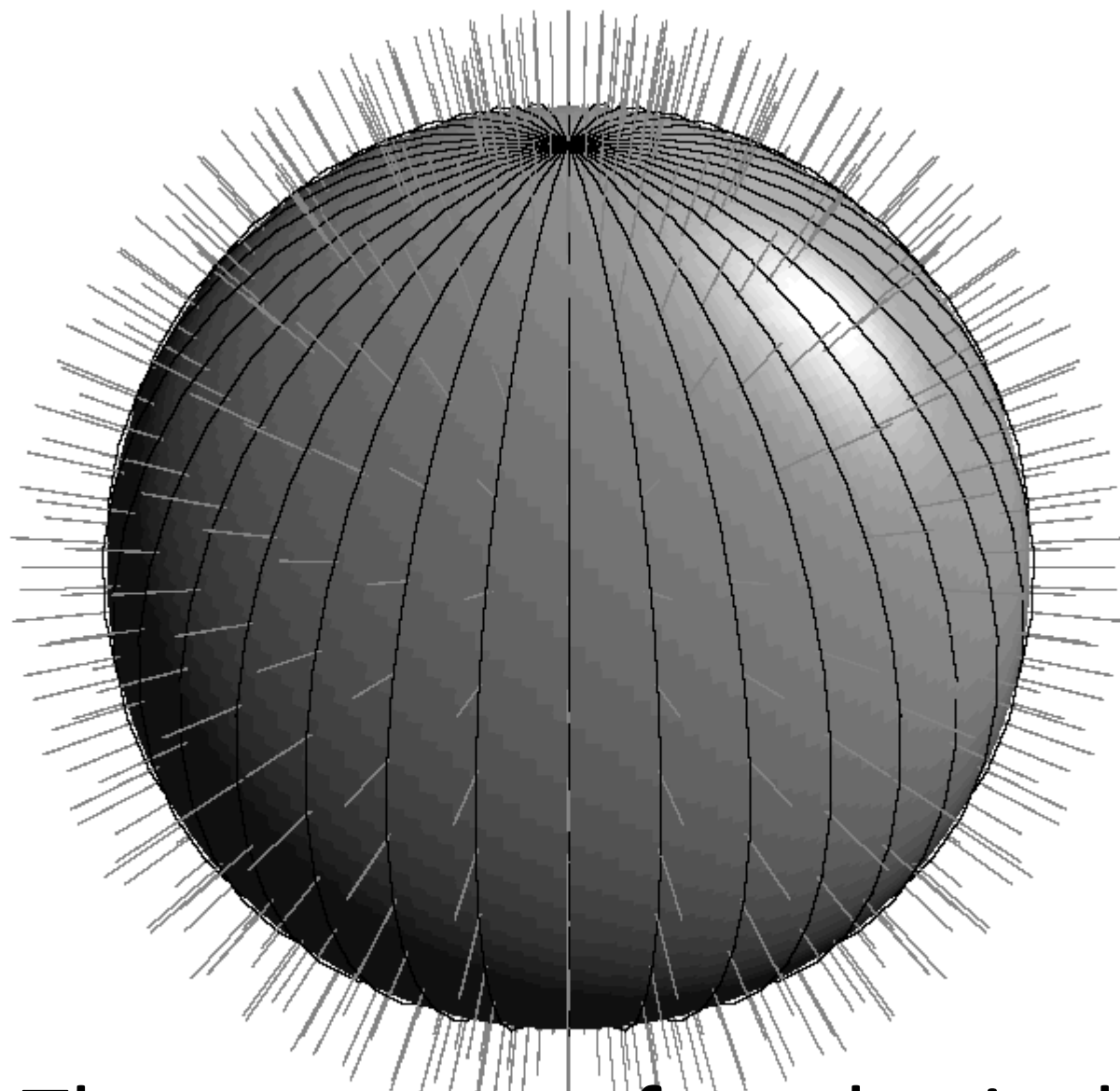
Are you spending a lot of time calculating convolutions on the sphere?

- Object detection
- PDE solver (pseudo-spectral methods)
- Optimal filtering
- Simulating random fields on the sphere
- Wavelet decompositions (including asymmetric, steerable)
- Optical smoothing in simulations
- Power spectrum inference, Wiener filtering:

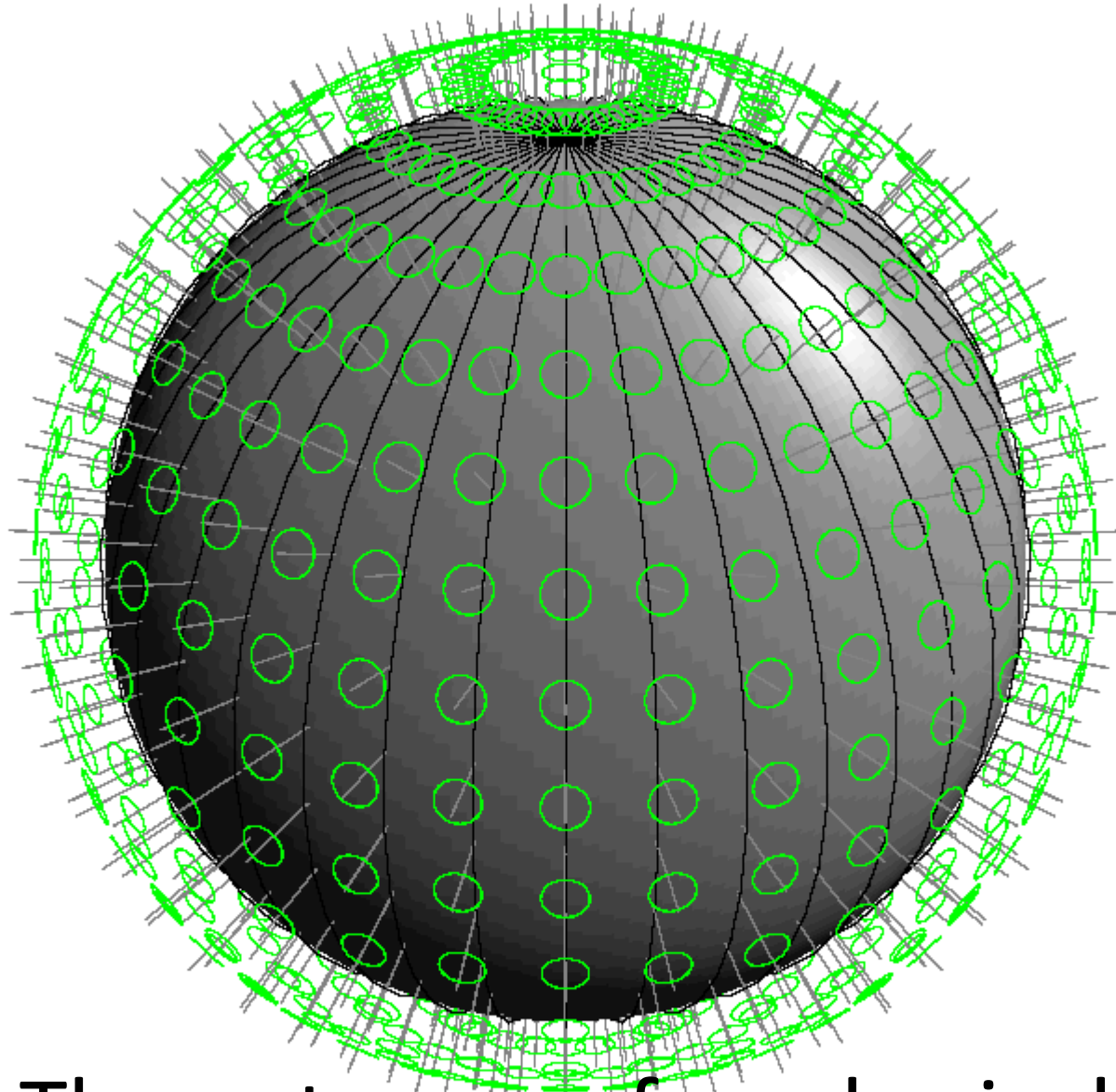
$$\left(S^{-1} + \sum_{\text{channels}} \text{B}_i N^{-1} \text{B}_i \right) m = \left(\sum_{\text{channels}} \text{B}_i N^{-1} \text{B}_i \right) d$$



The outcome of a spherical convolution is a function over $SO(3)$



The outcome of a spherical convolution is a function over $SO(3)$



The outcome of a spherical convolution is a function over $SO(3)$

Accelerating spherical convolution

In general, convolution on the sphere can be written as

$$T(\Phi_2, \Theta, \Phi_1) = \int d\Omega [\hat{D}(\Phi_2, \Theta, \Phi_1)b](\vec{\gamma})^* s(\vec{\gamma})$$

This expression takes of order L^5
operations to compute:

The key step leading to massively accelerated convolution
is the factorisation of the rotation operator (Risbo 1996)

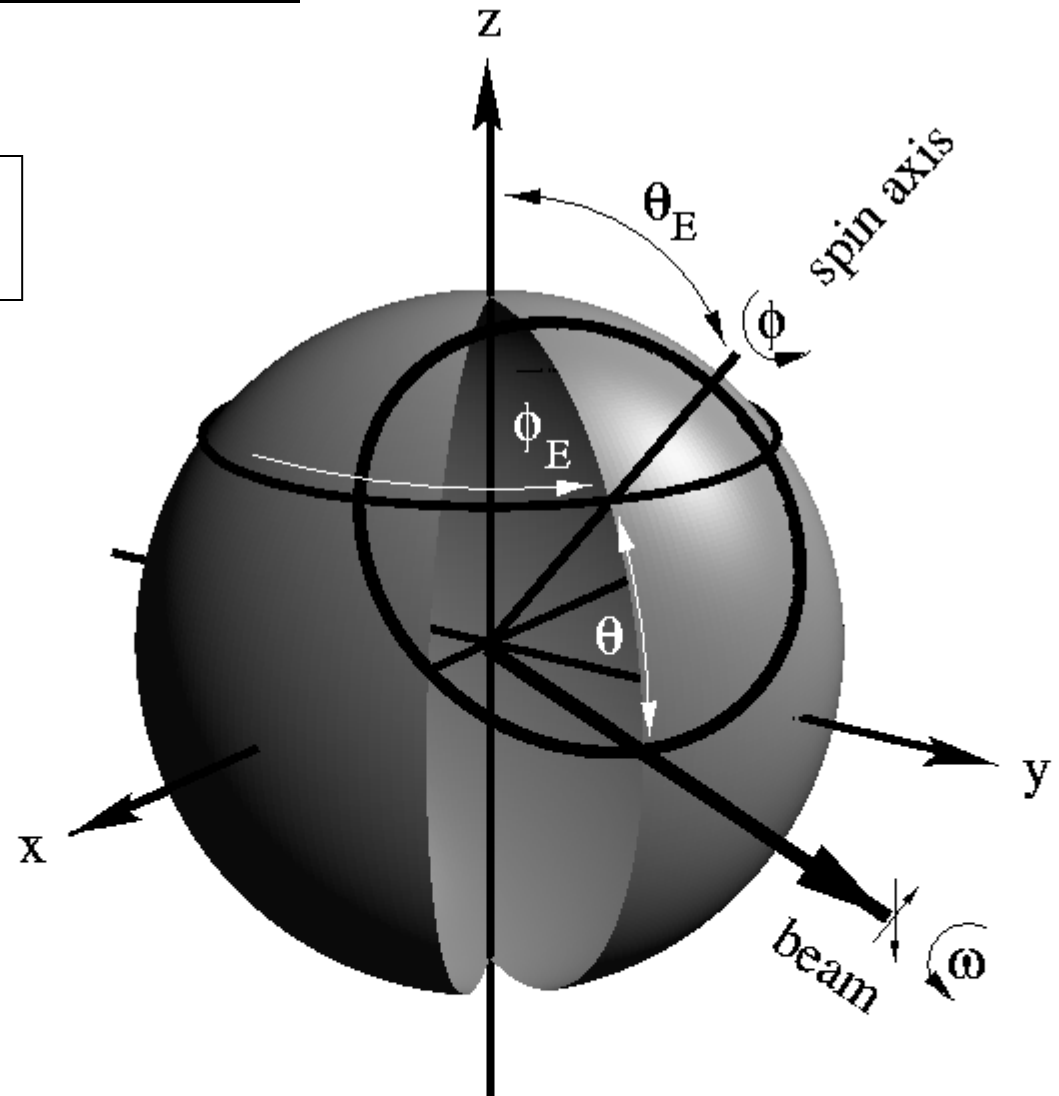
$$\hat{D}(\Phi_2, \Theta, \Phi_1) \equiv \hat{D}(\phi_E, \theta_E, 0)\hat{D}(\phi, \theta, \omega)$$

$$T(\phi_E, \phi, \omega) = \int d\Omega [\hat{D}(\phi_E, \theta_E, 0)\hat{D}(\phi, \theta, \omega)b](\vec{\gamma})^* s(\vec{\gamma})$$

Convolution Coordinates

$$\hat{D}(\Phi_2, \Theta, \Phi_1) \equiv \hat{D}(\phi_E, \theta_E, 0) \hat{D}(\phi, \theta, \omega)$$

This factorisation corresponds to moving the beam into place using two successive rotations.



Accelerating spherical convolution II

$$\hat{D}(\Phi_2, \Theta, \Phi_1) \equiv \hat{D}(\phi_E, \theta_E, 0) \hat{D}(\phi, \theta, \omega)$$

$$T(\phi_E, \phi, \omega) = \int d\Omega [\hat{D}(\phi_E, \theta_E, 0) \hat{D}(\phi, \theta, \omega) b](\vec{\gamma})^* s(\vec{\gamma})$$

The special property of this factorisation is that the Fourier transform of the convolution takes only $O(L^4)$ operations to compute!

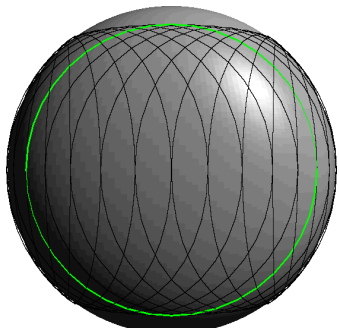
$$T_{m m' m''} = \sum_l s_{lm} a_{m M}^l(\theta_E) a_{M M'}^l(\theta) b_{l M'}^*$$

There are special cases which reduce to $O(L^3)$:

1) Basic Scan Paths (Ring Torus)

$$T_{m m'}(\omega = 0) = \sum_l s_{lm} a_{m m'}^l(\theta_E) X_{l m'}$$

$$X_{l m} \equiv \sum_M a_{m M}^l(\theta) b_{l M}^*$$



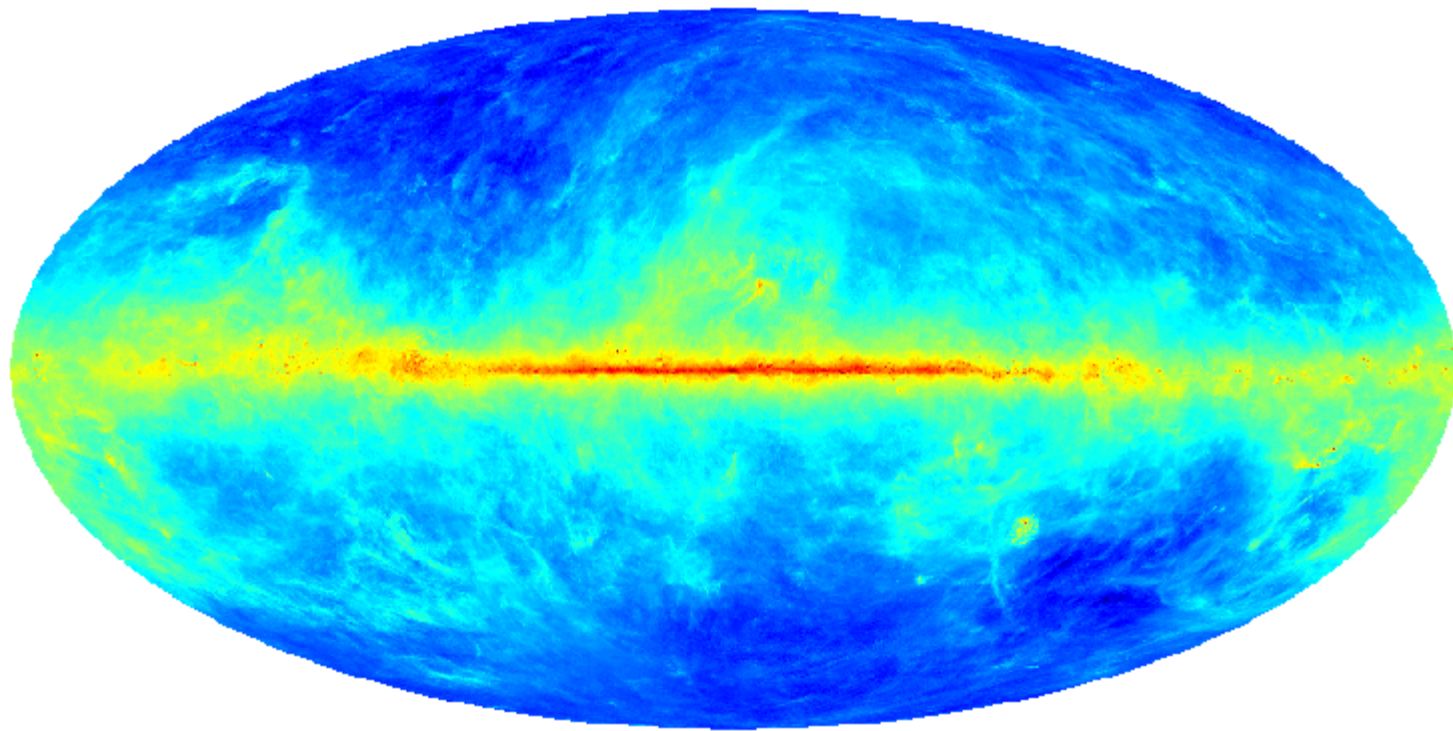
2) Azimuthally symmetric beam

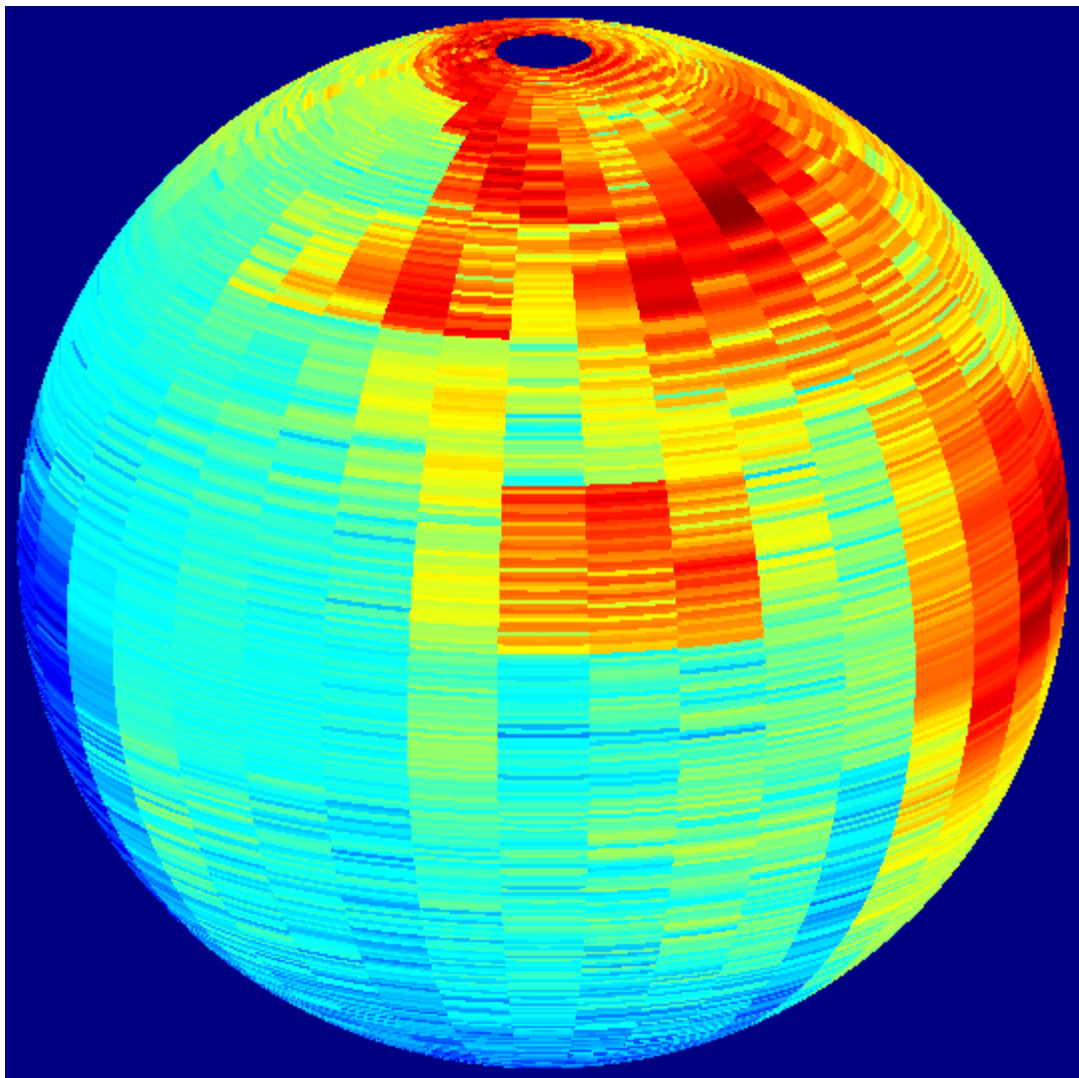
reduces to standard formula

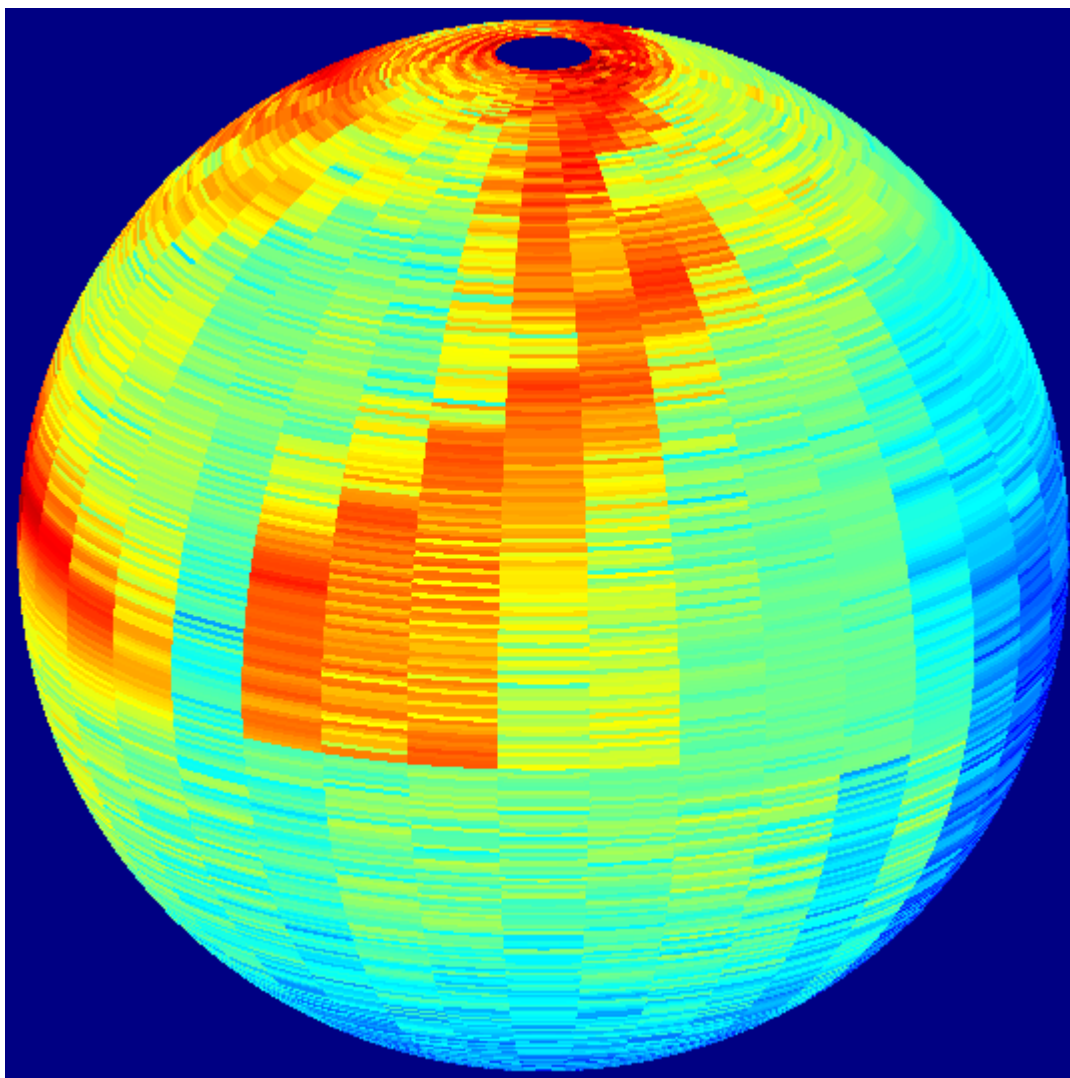
$$T(\phi_E, \phi) = \sum_{lm} Y_{lm}(\pi - \phi, \phi_E + \pi/2) b_{l0} s_{lm} \sqrt{2l+1}$$

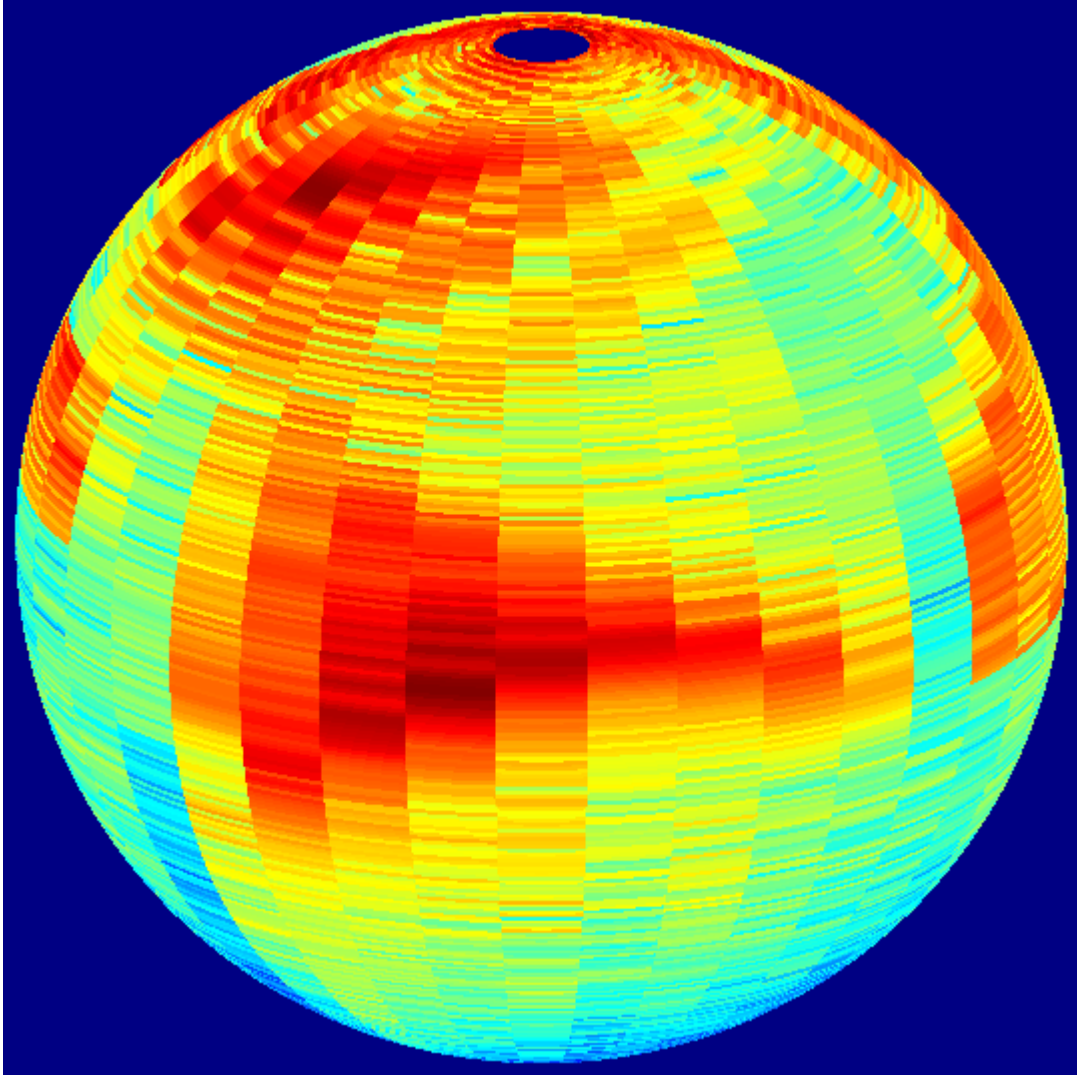
3) Low-order beam asymmetries $M' \ll L$

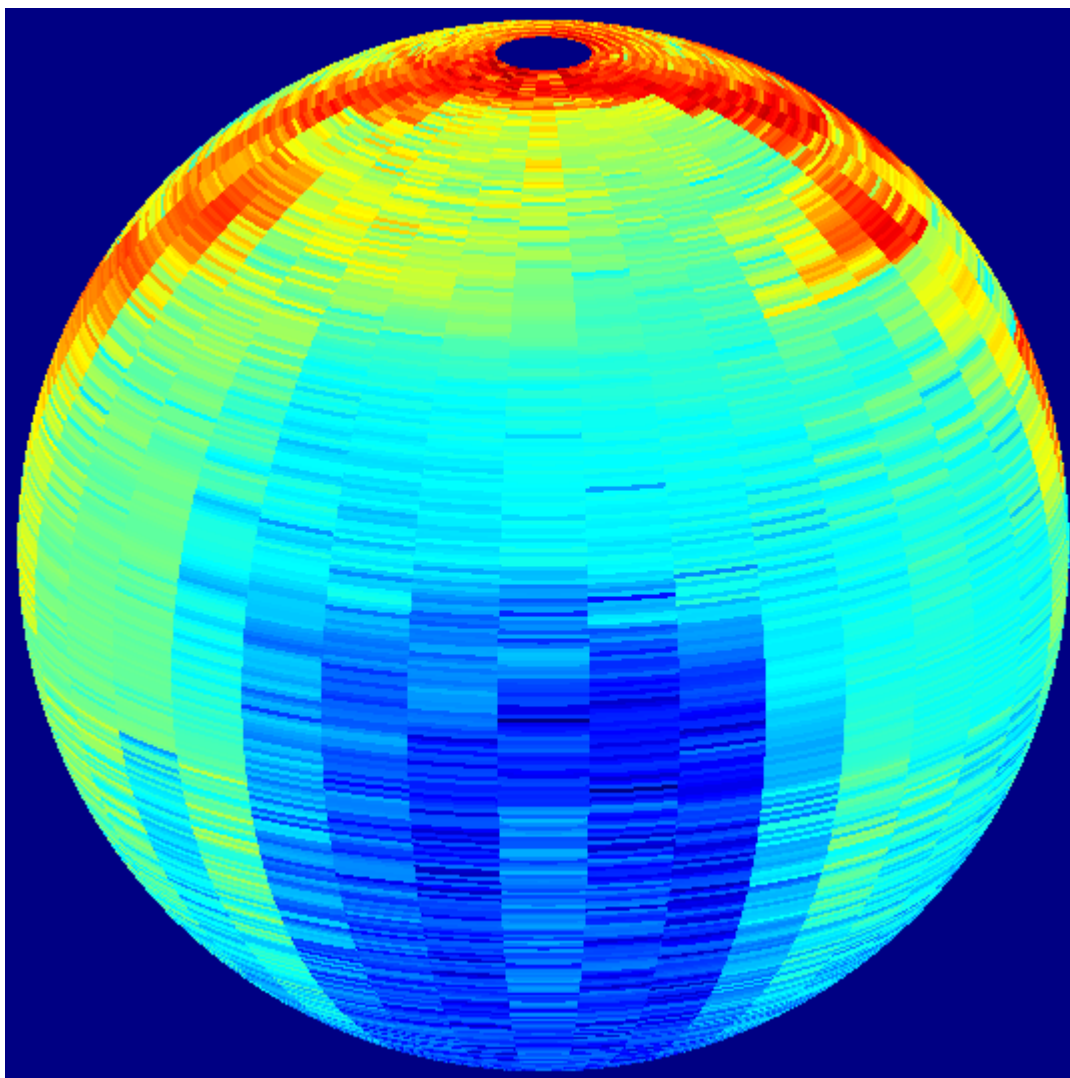
Example: Schlegel-Finkbeiner-Davis model of dust emission at 100GHz convolved with highly asymmetric physical beam model



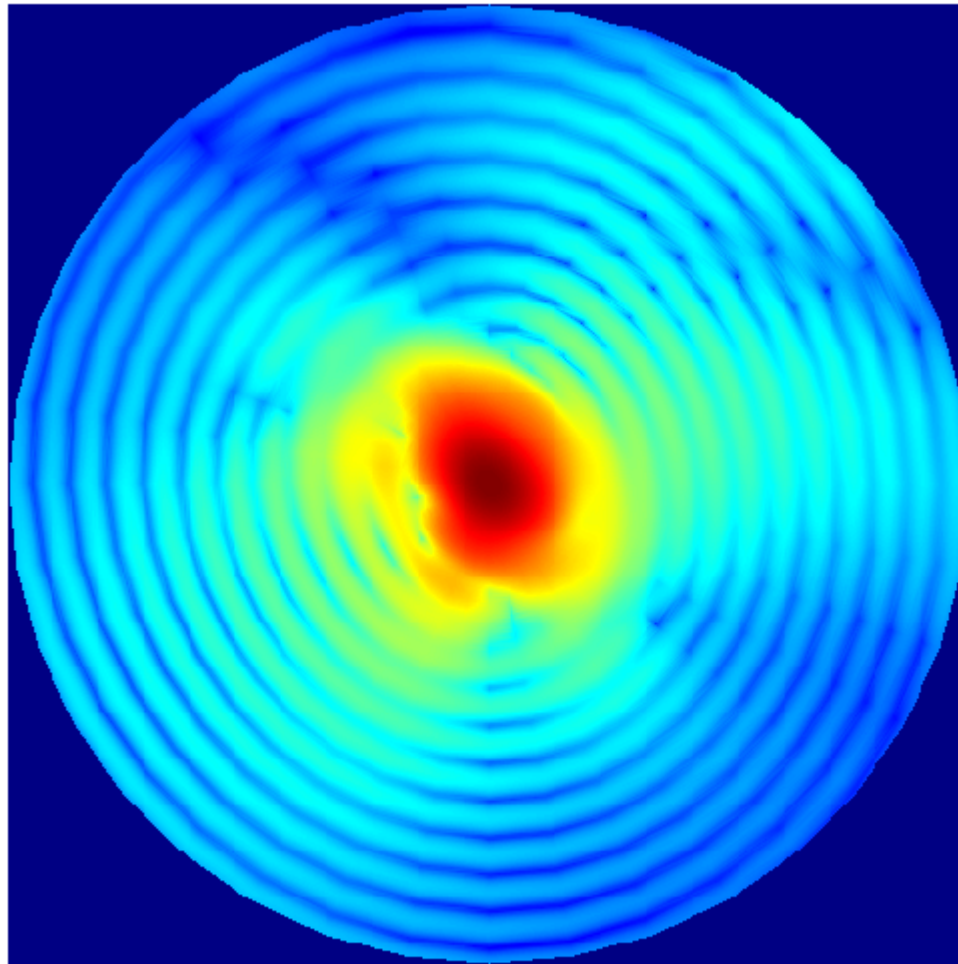








Central (main) beam

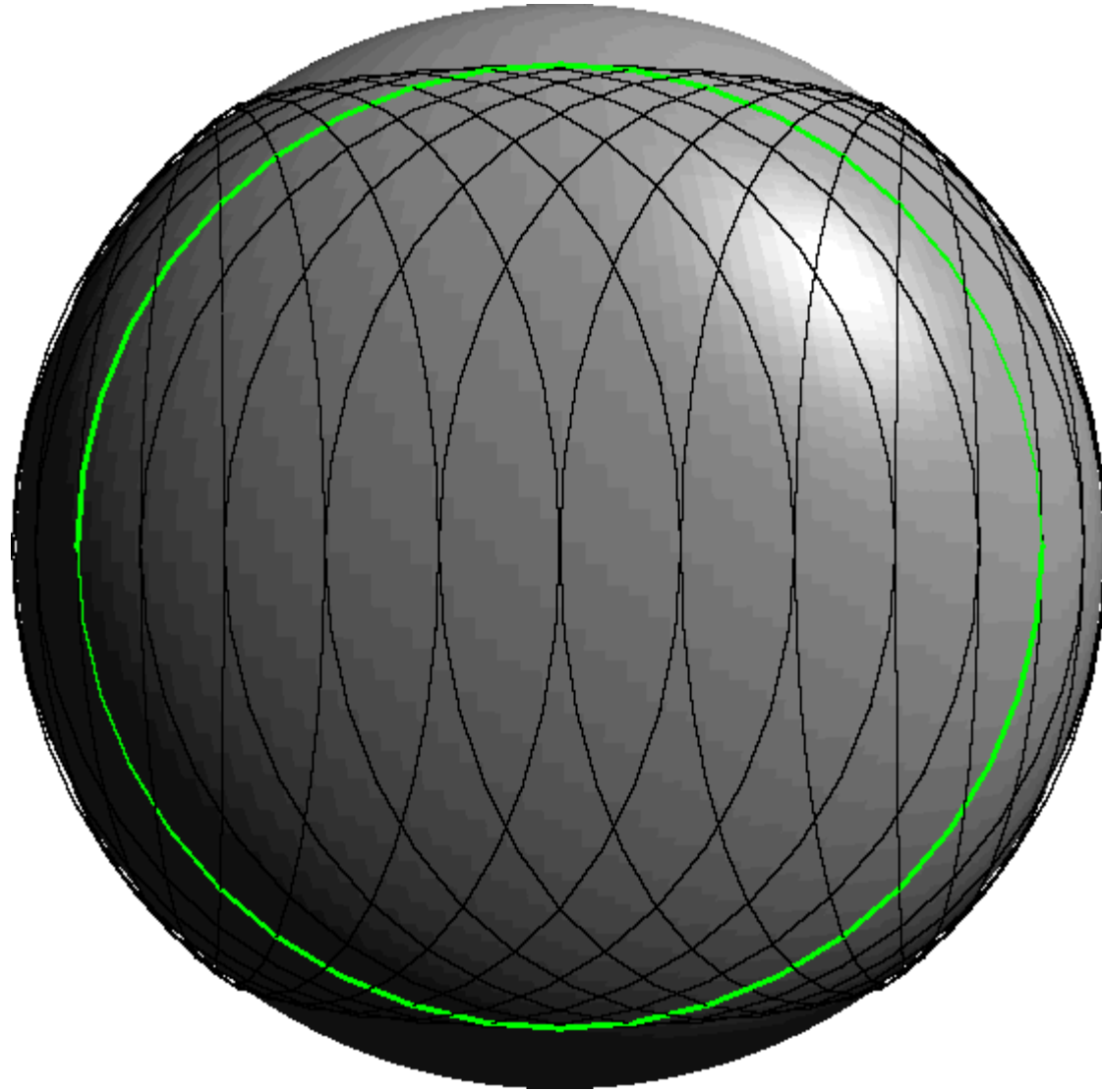


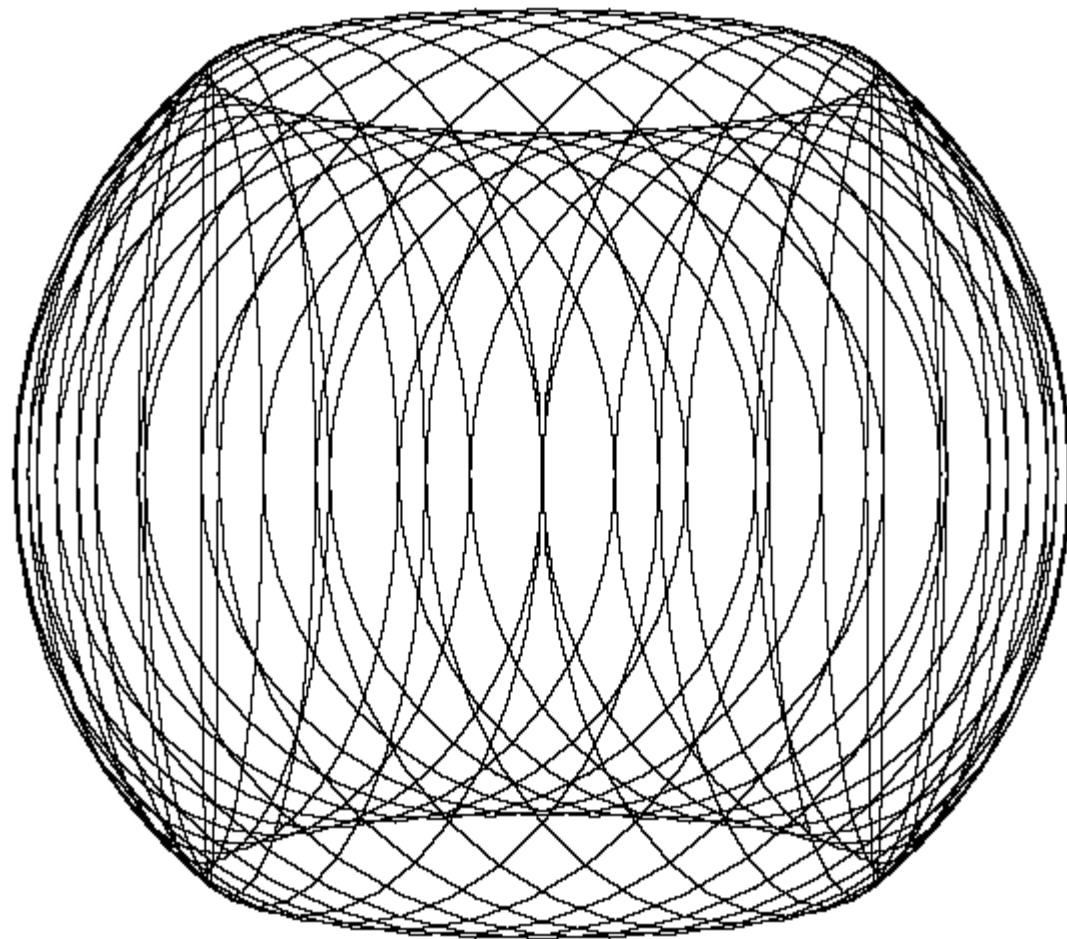
-80 dB

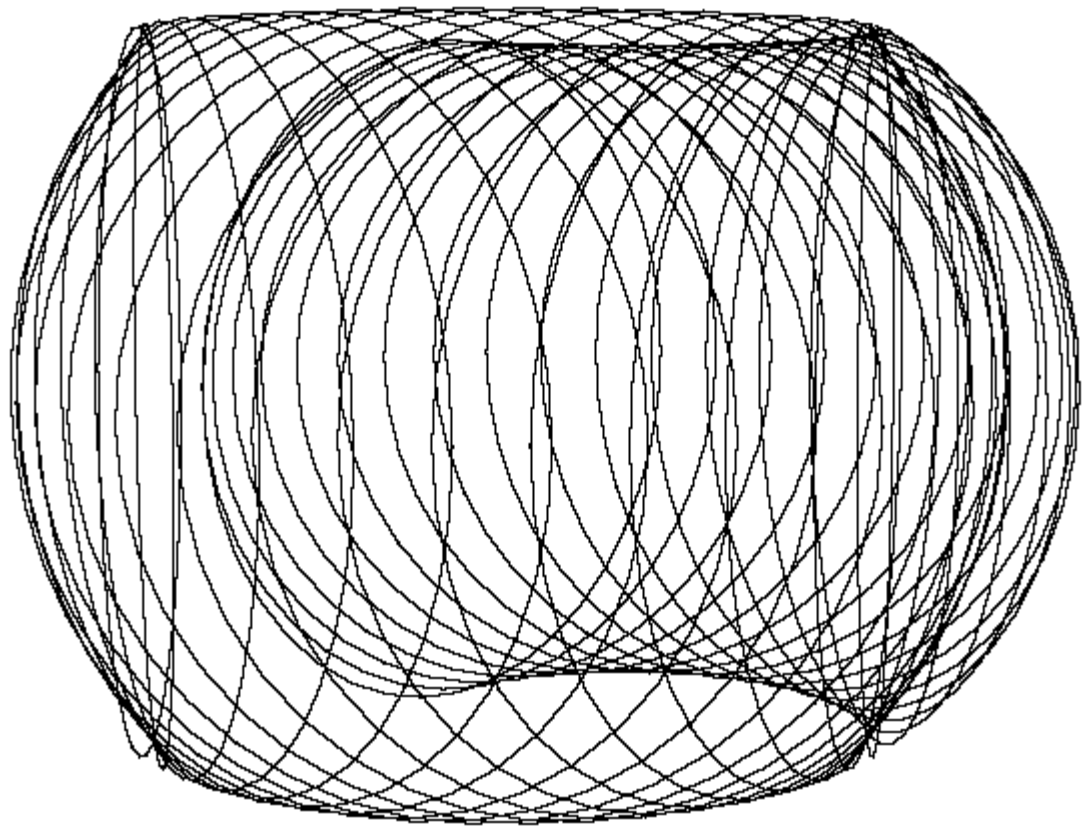


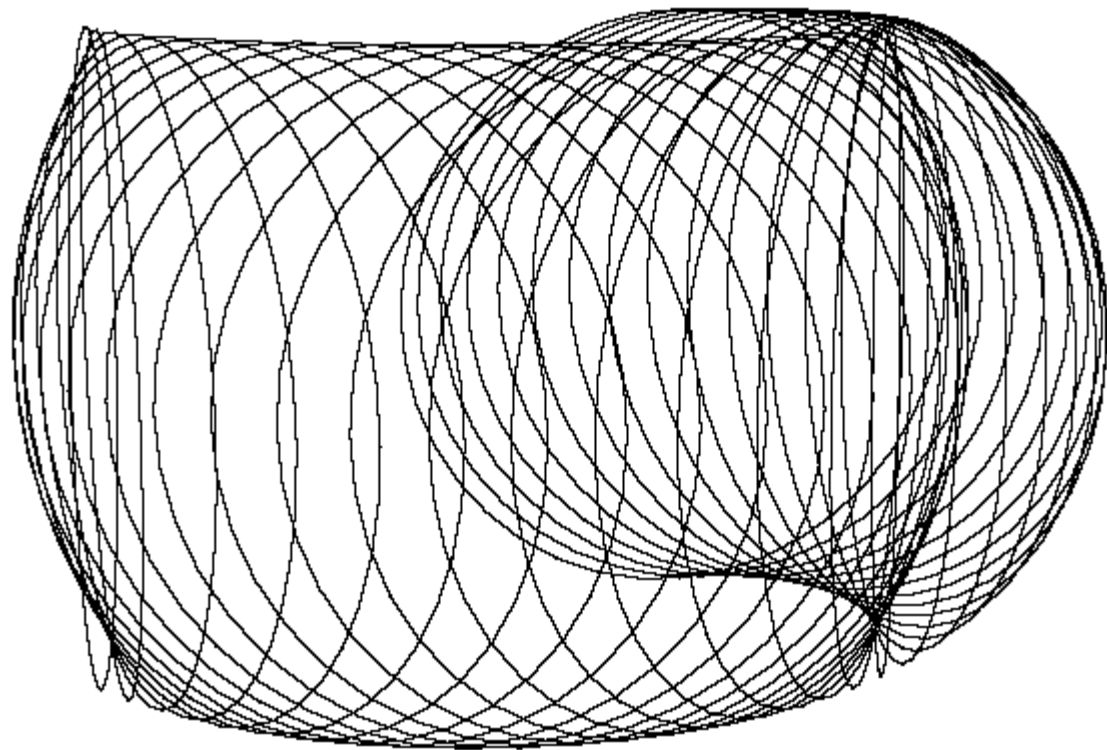
0 dB

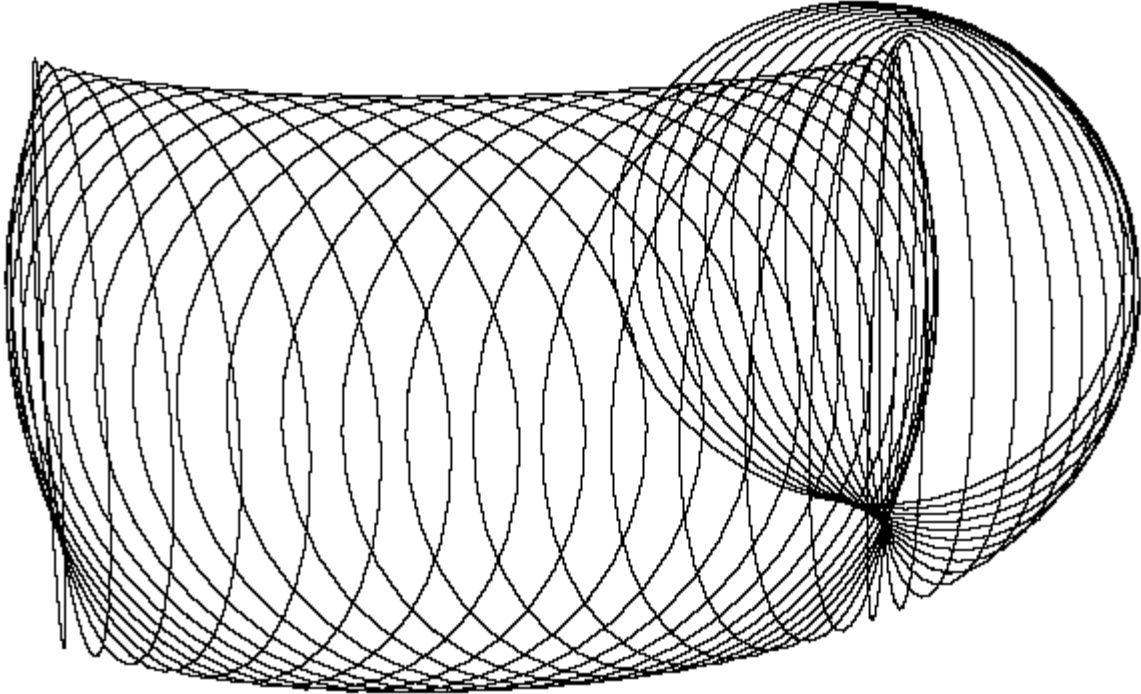
Basic Scan Path

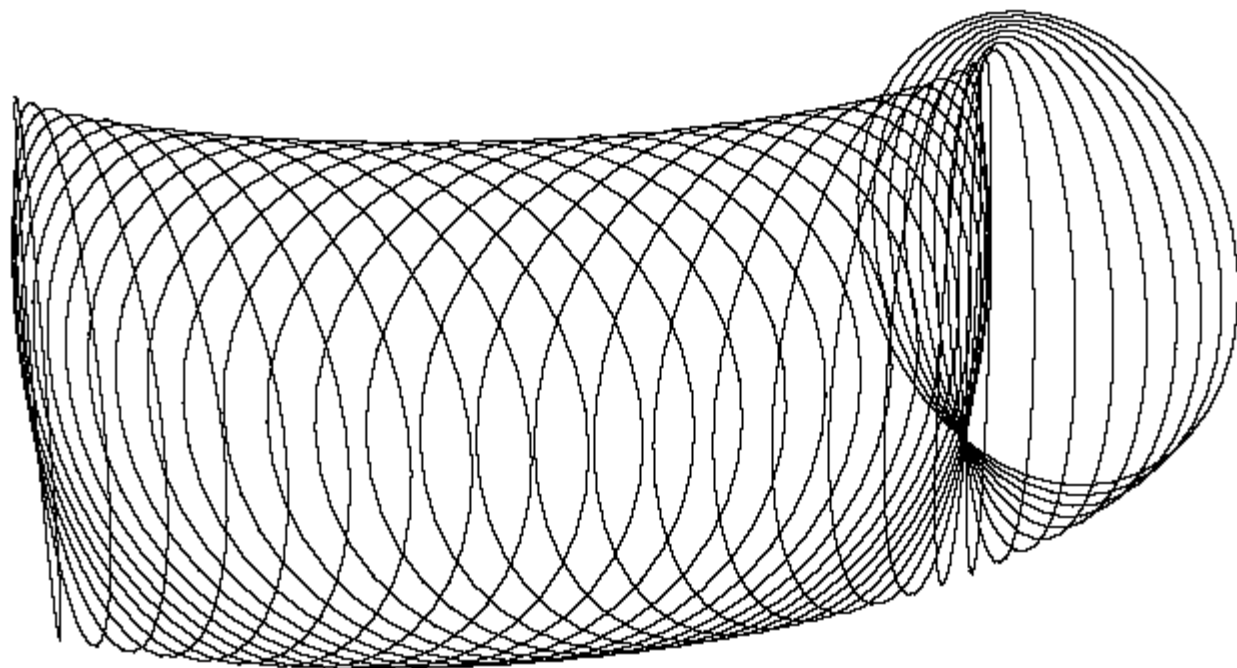


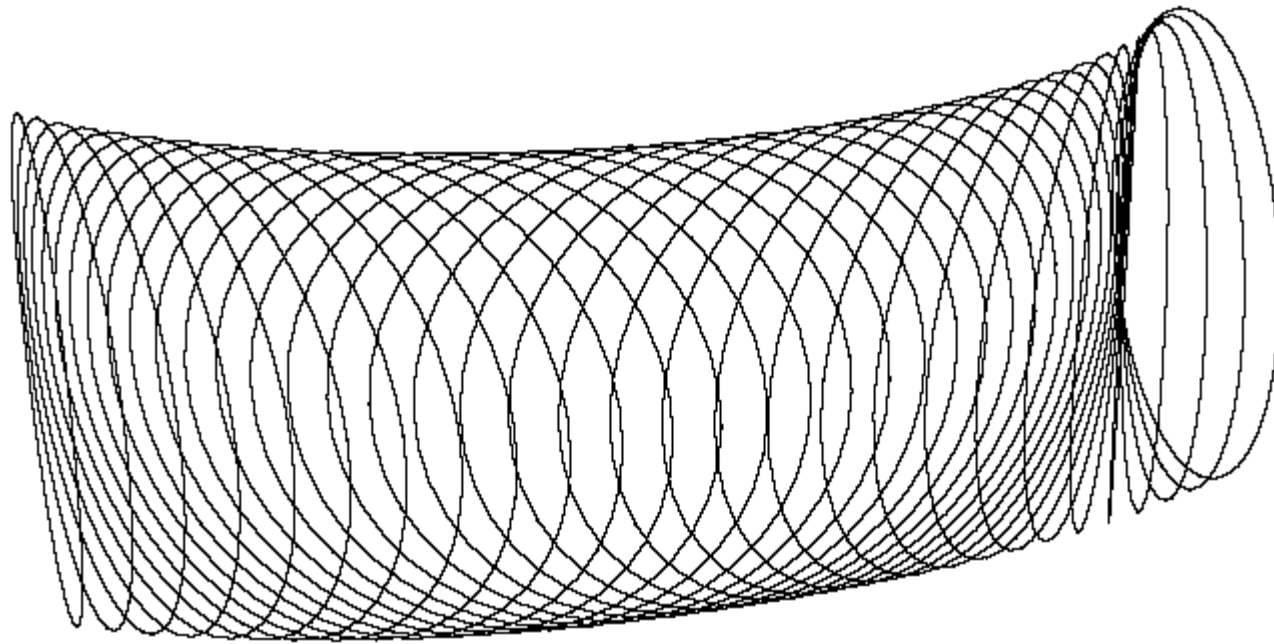


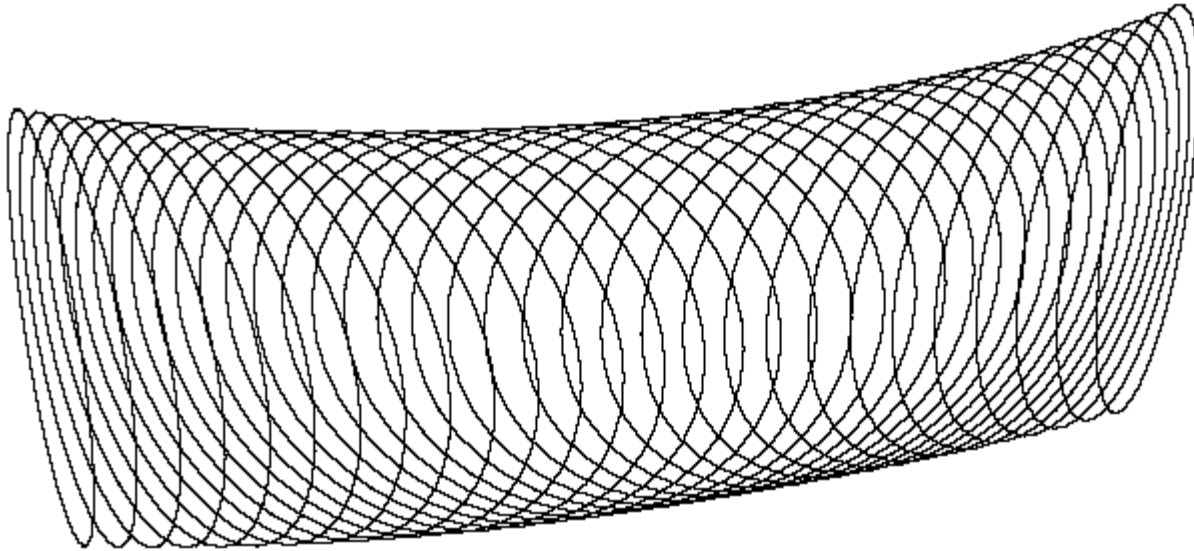


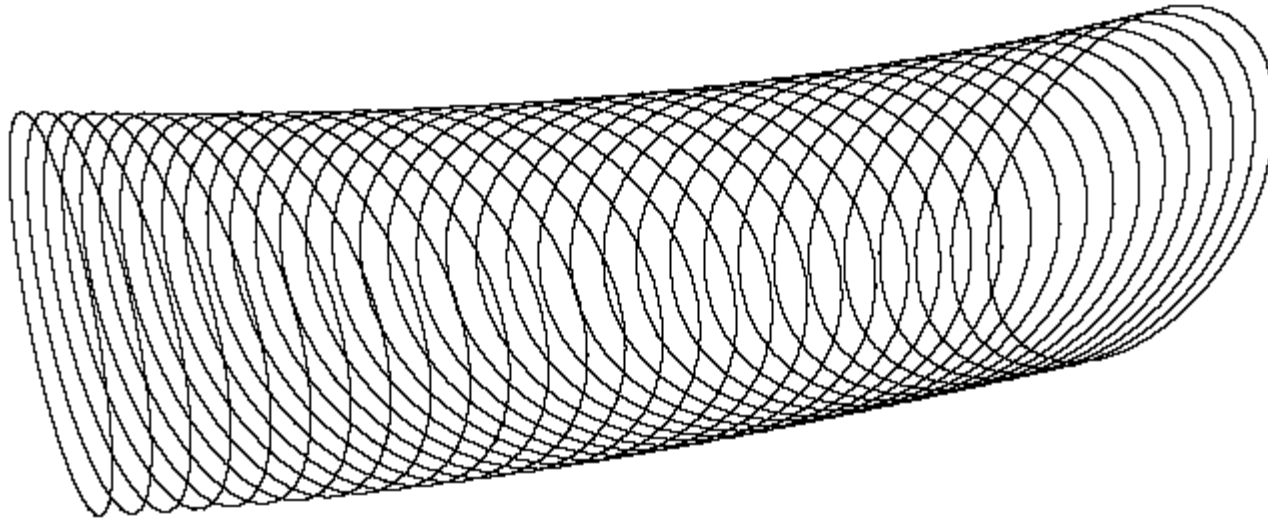


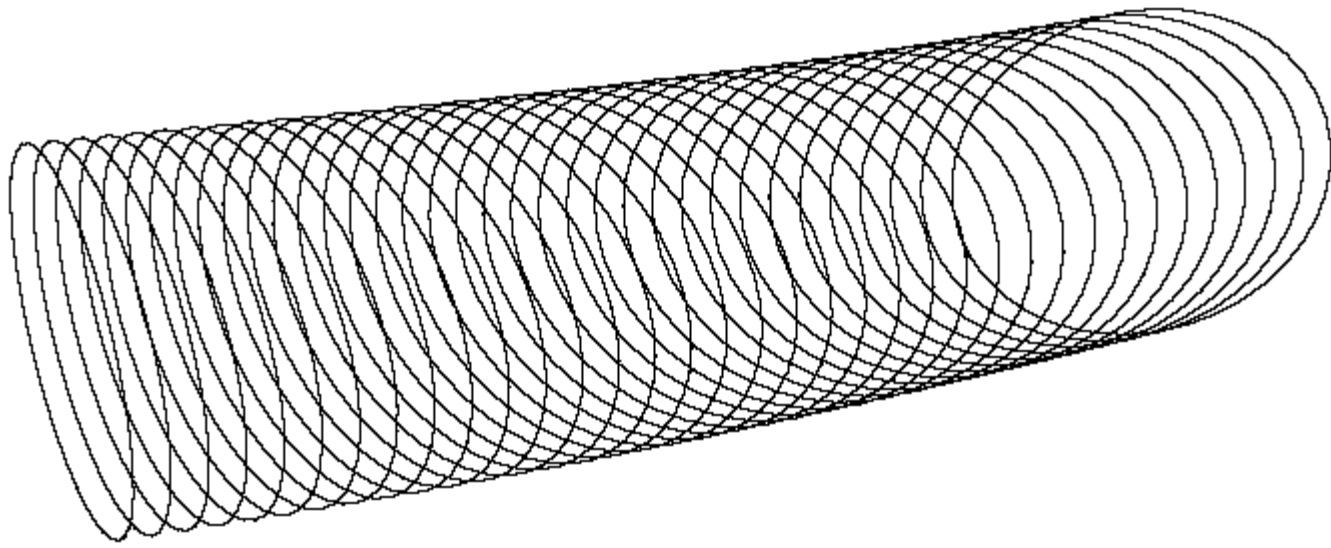


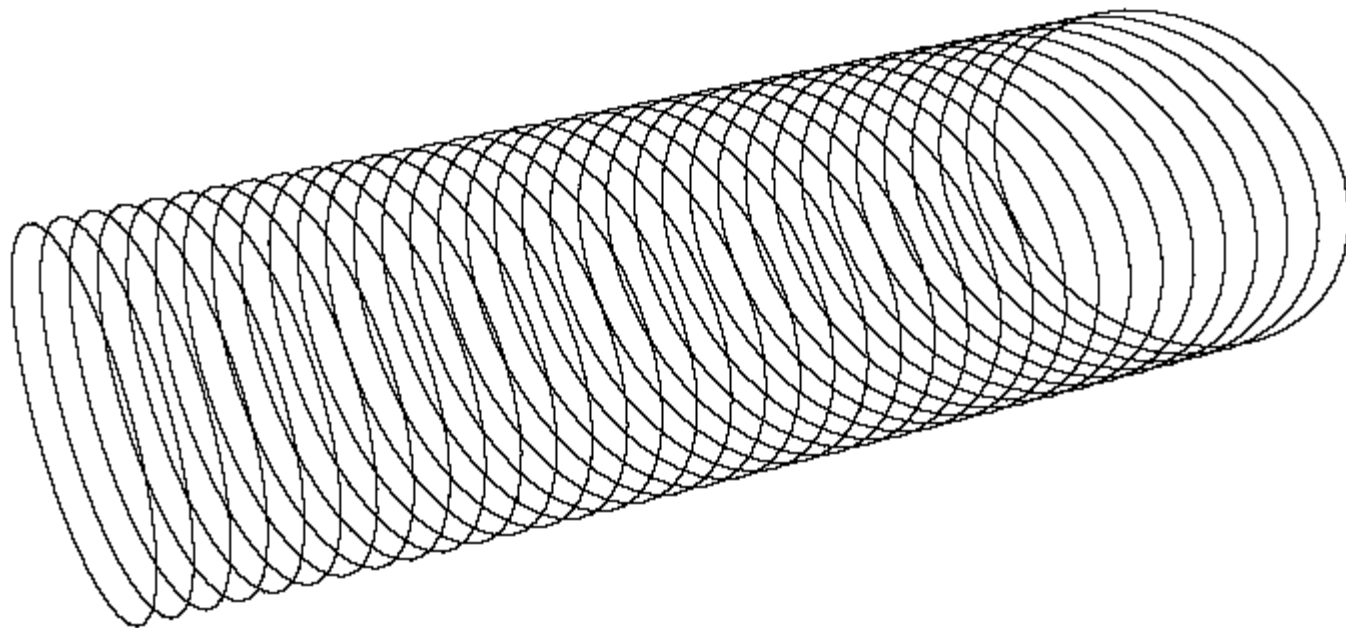


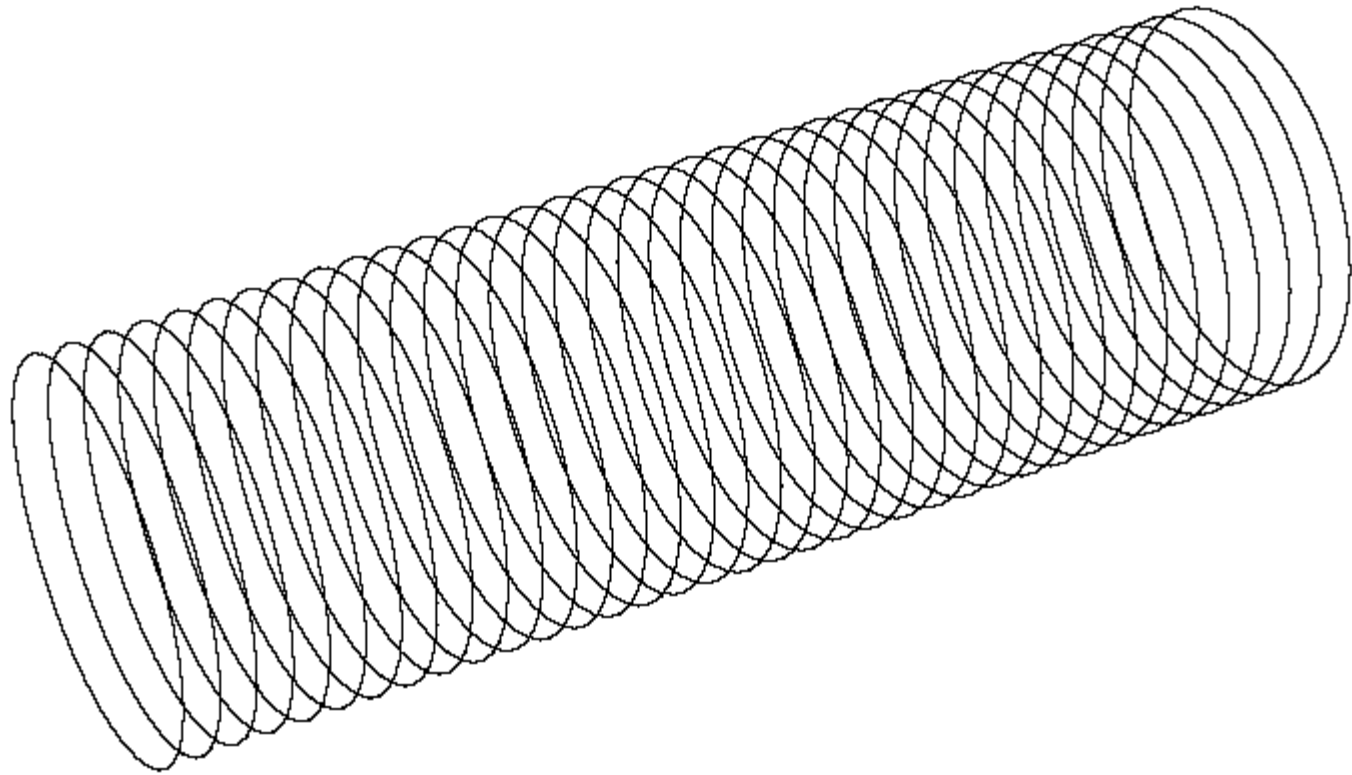


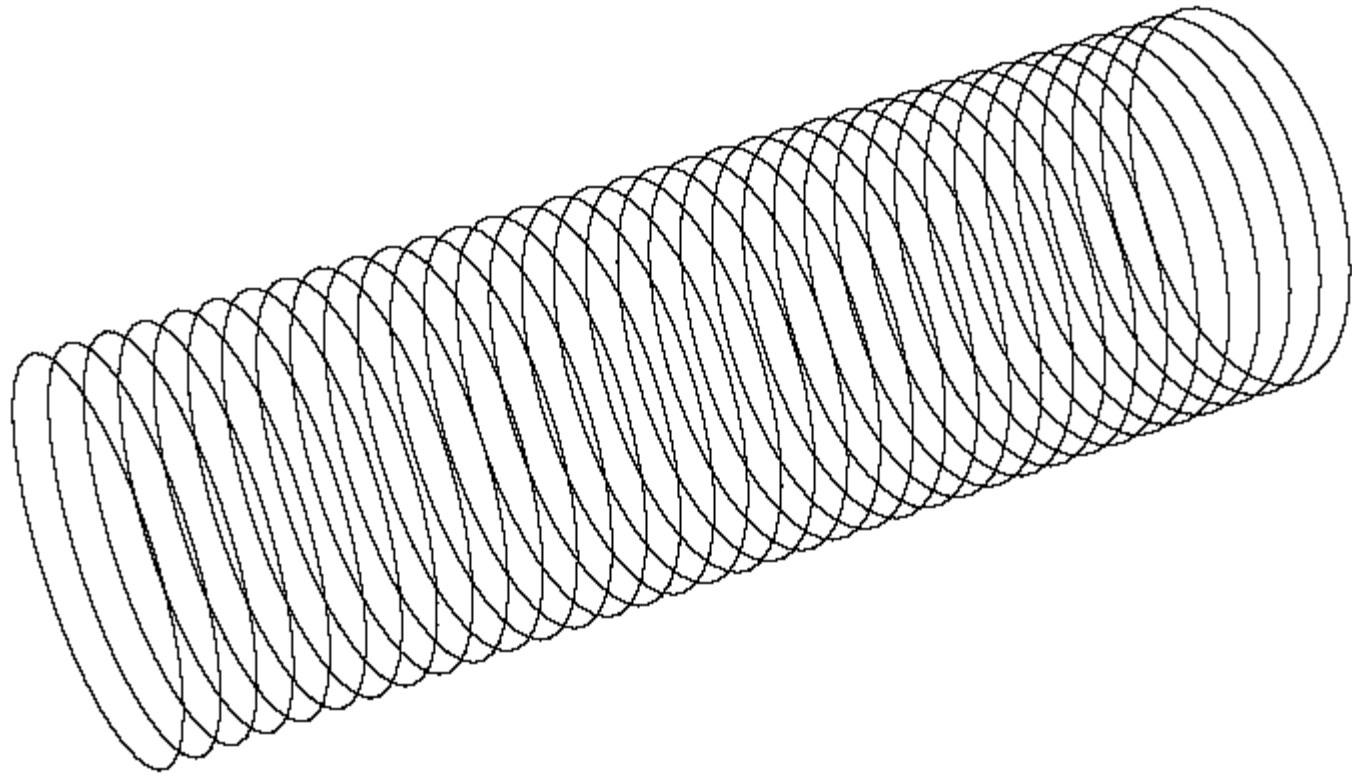


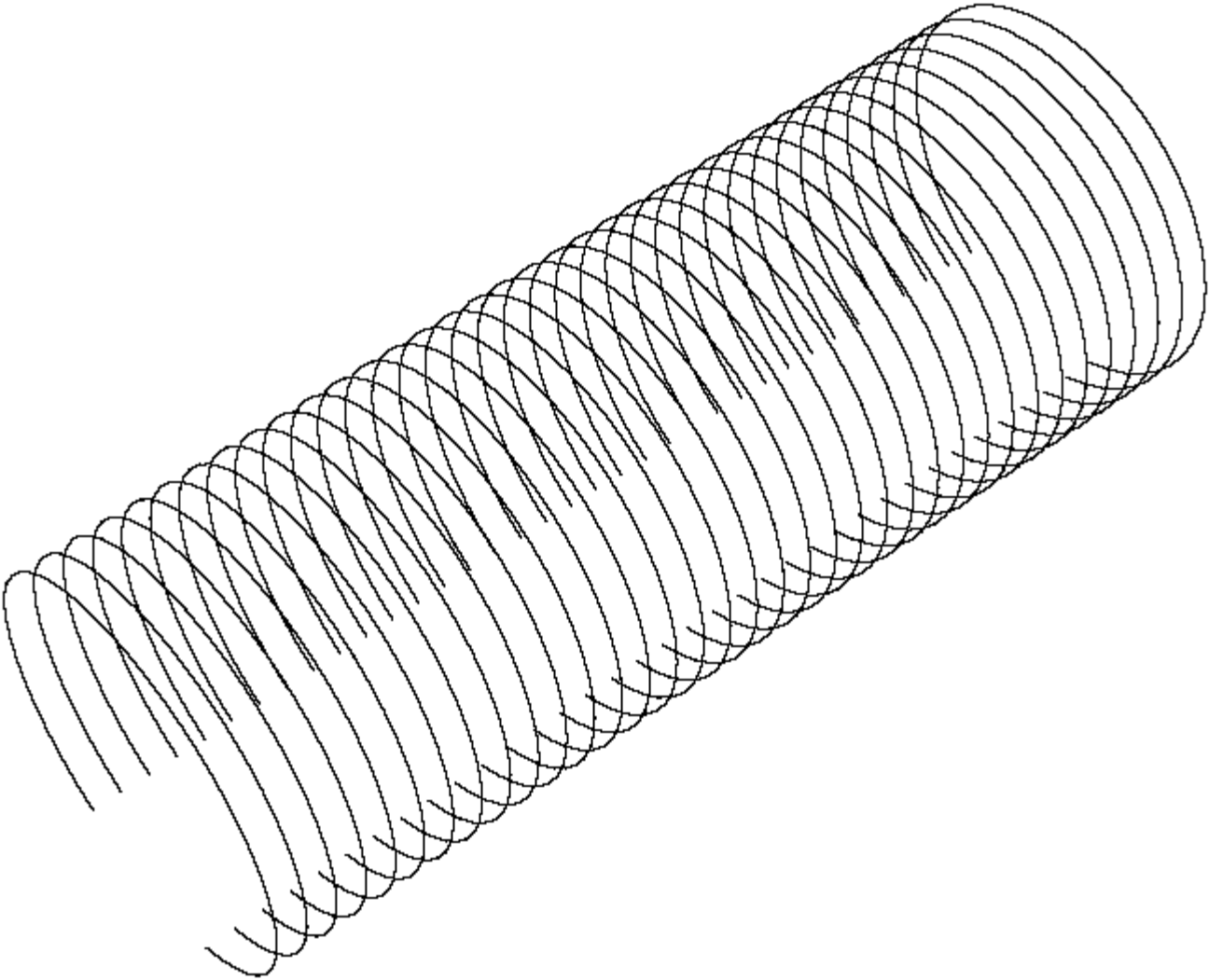


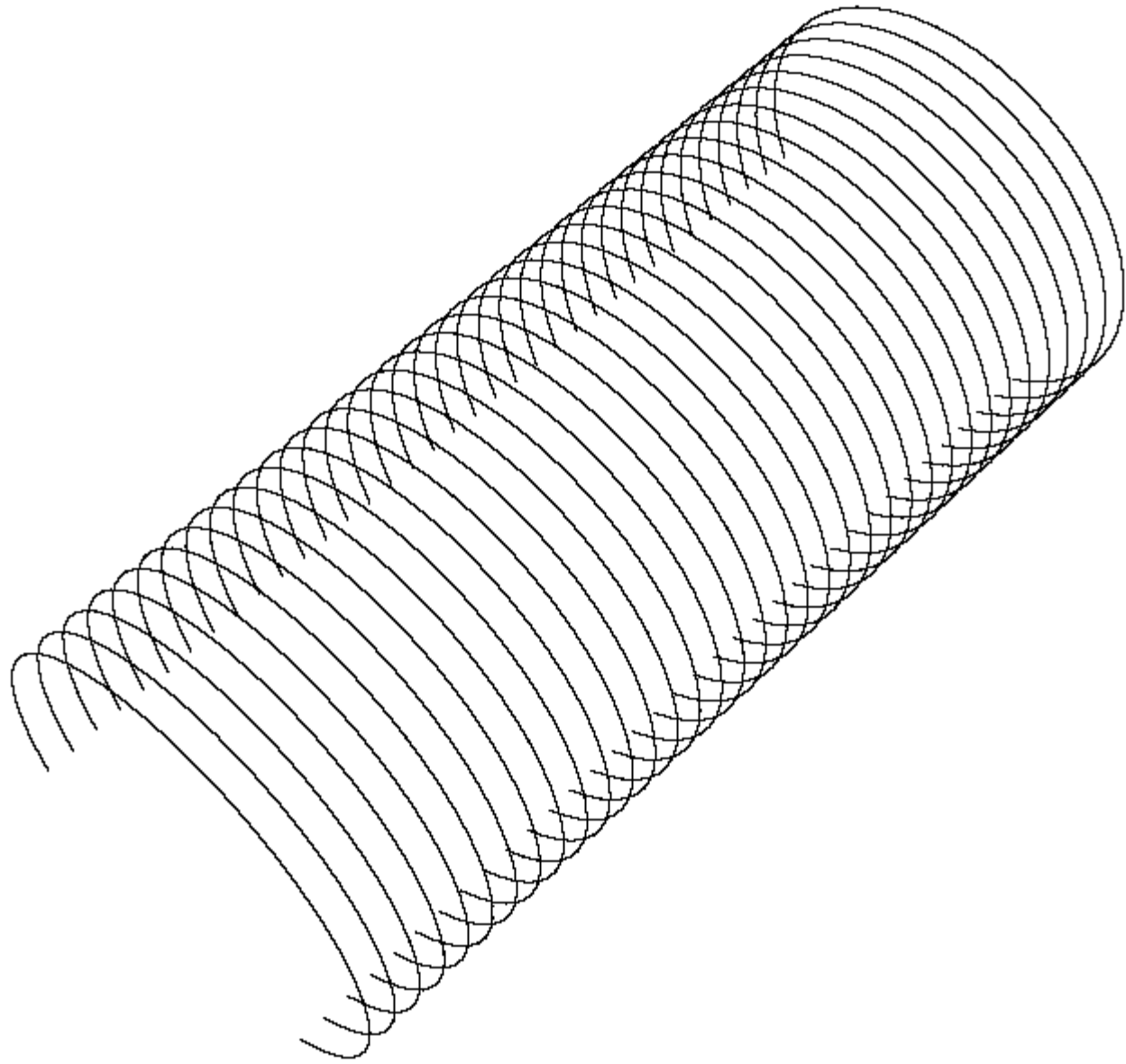


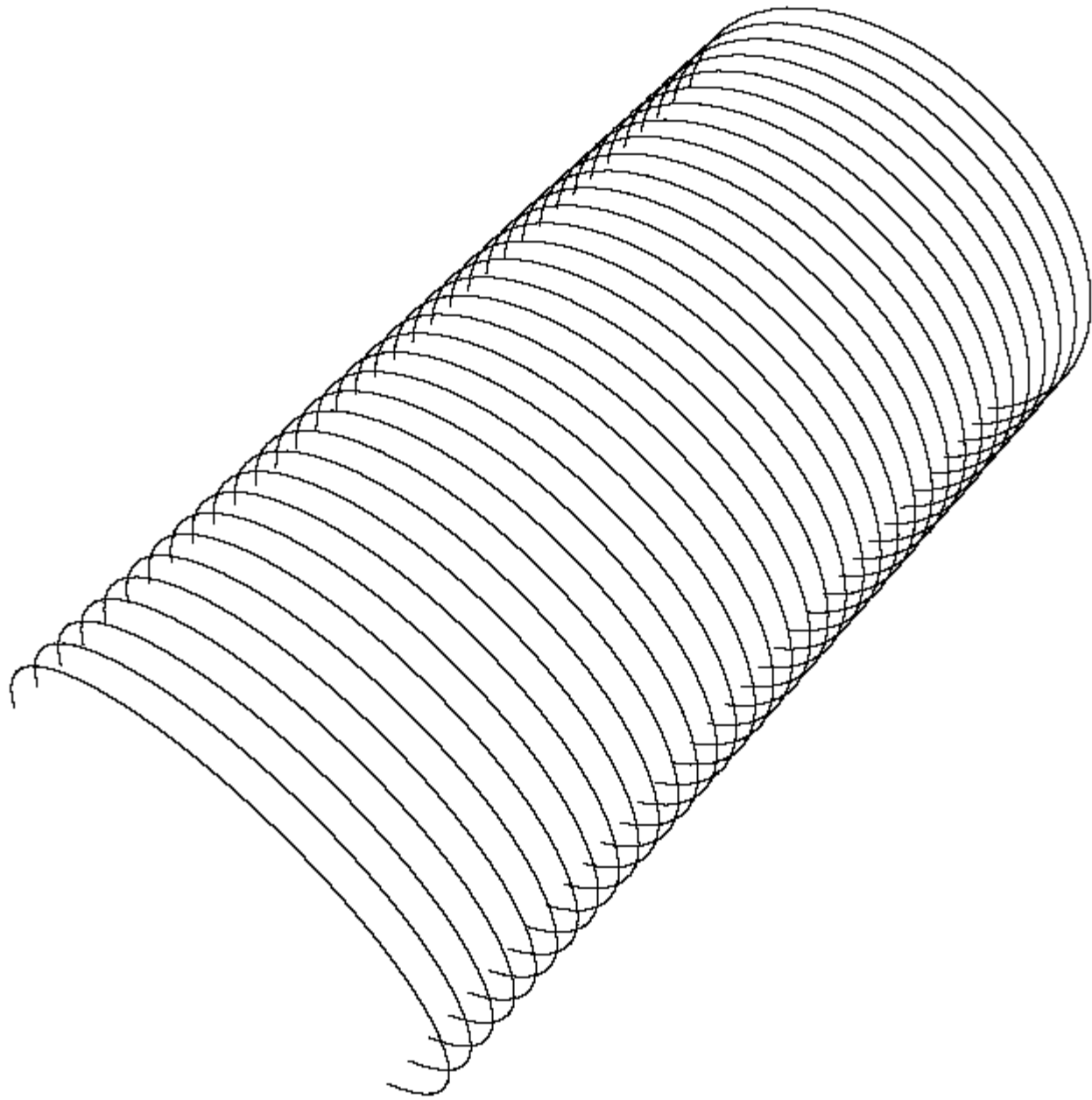


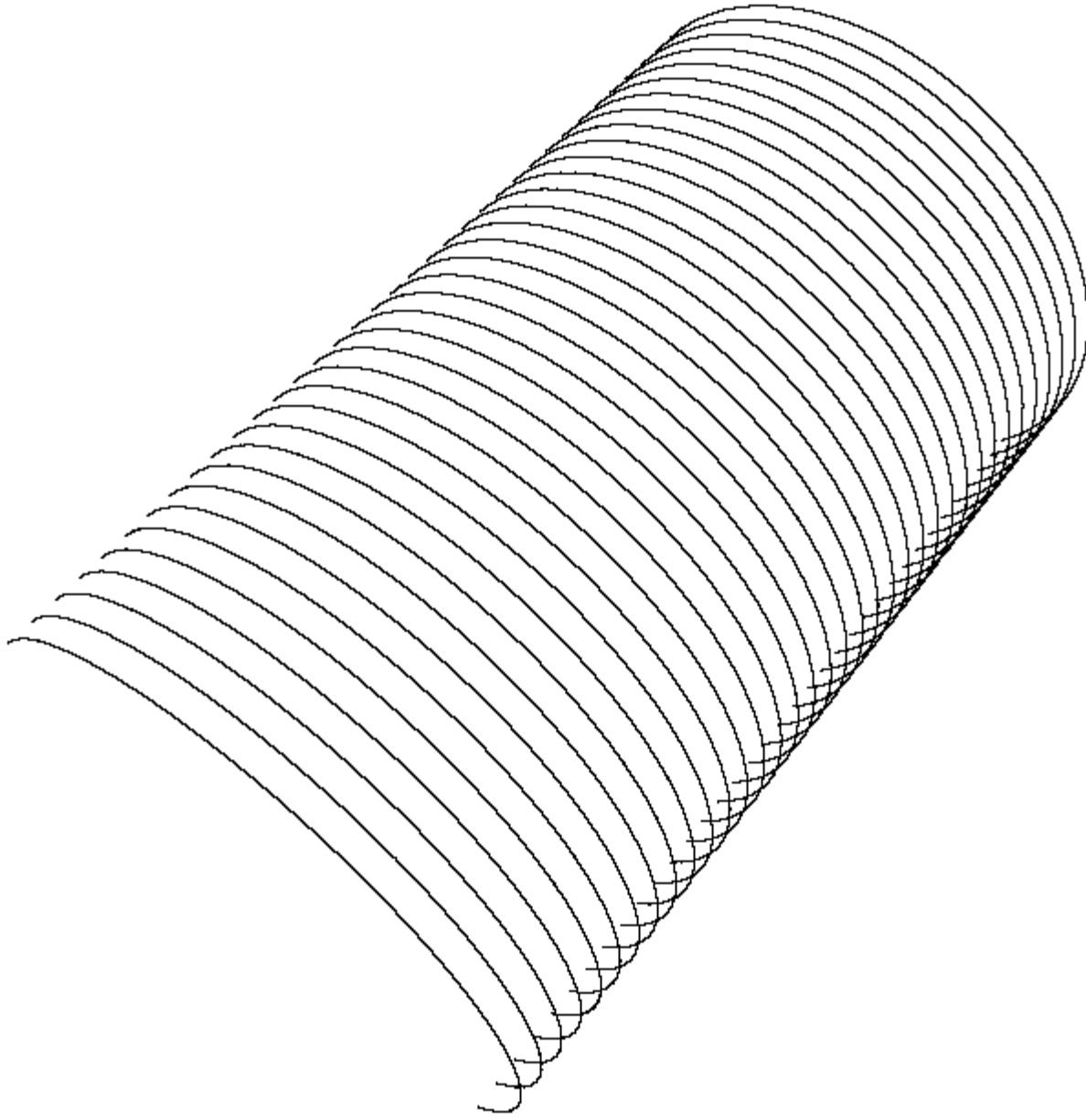


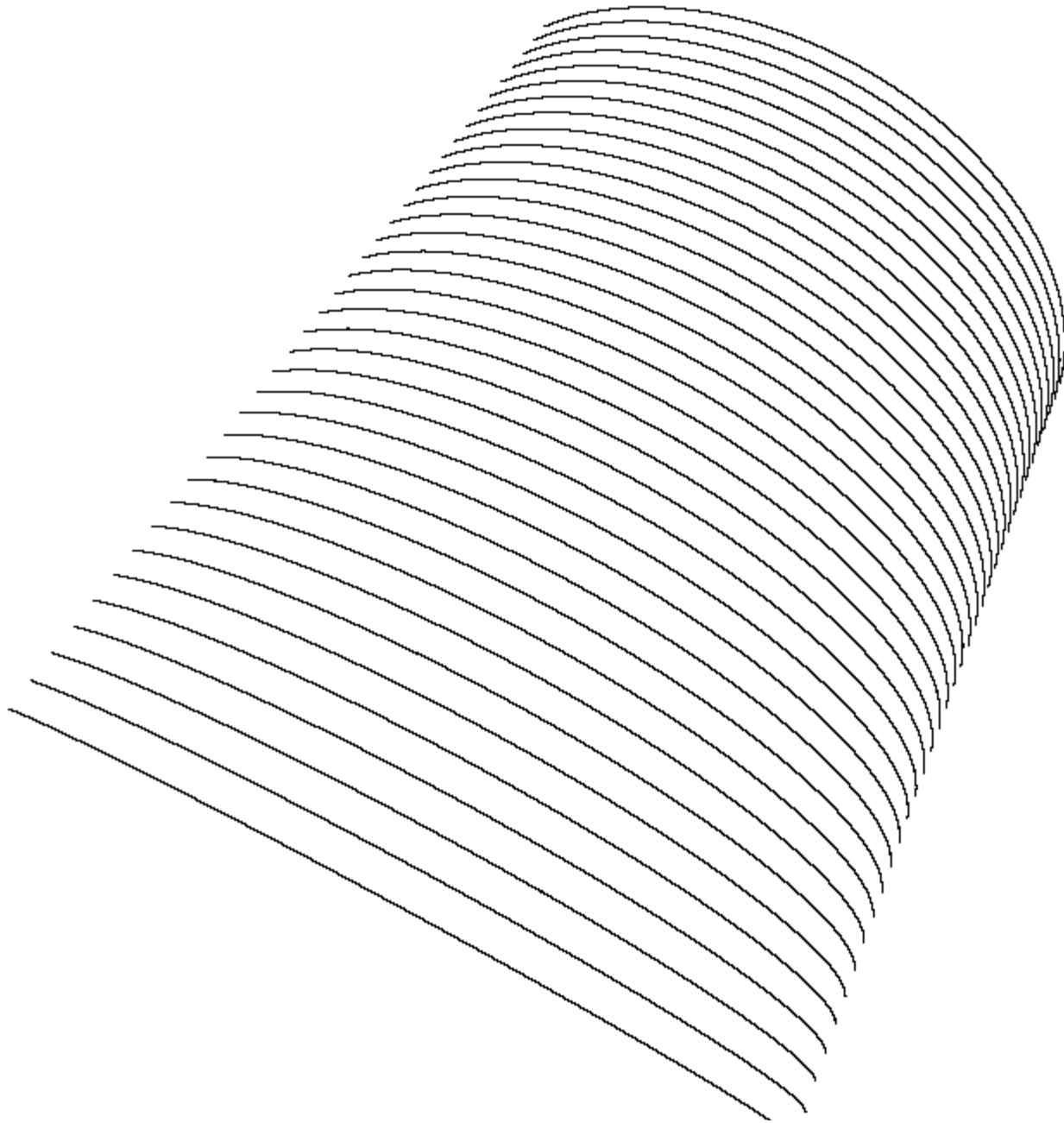


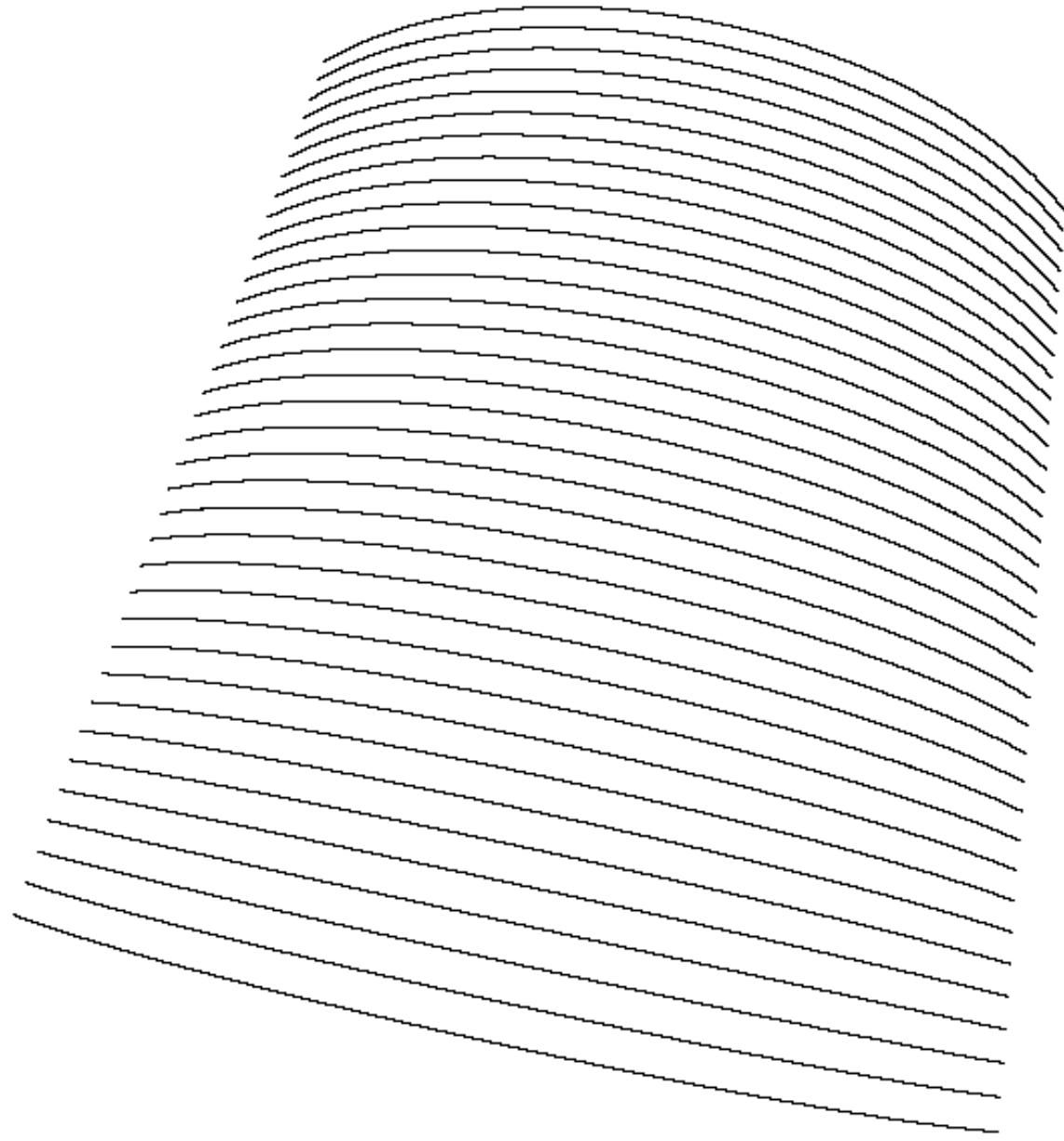


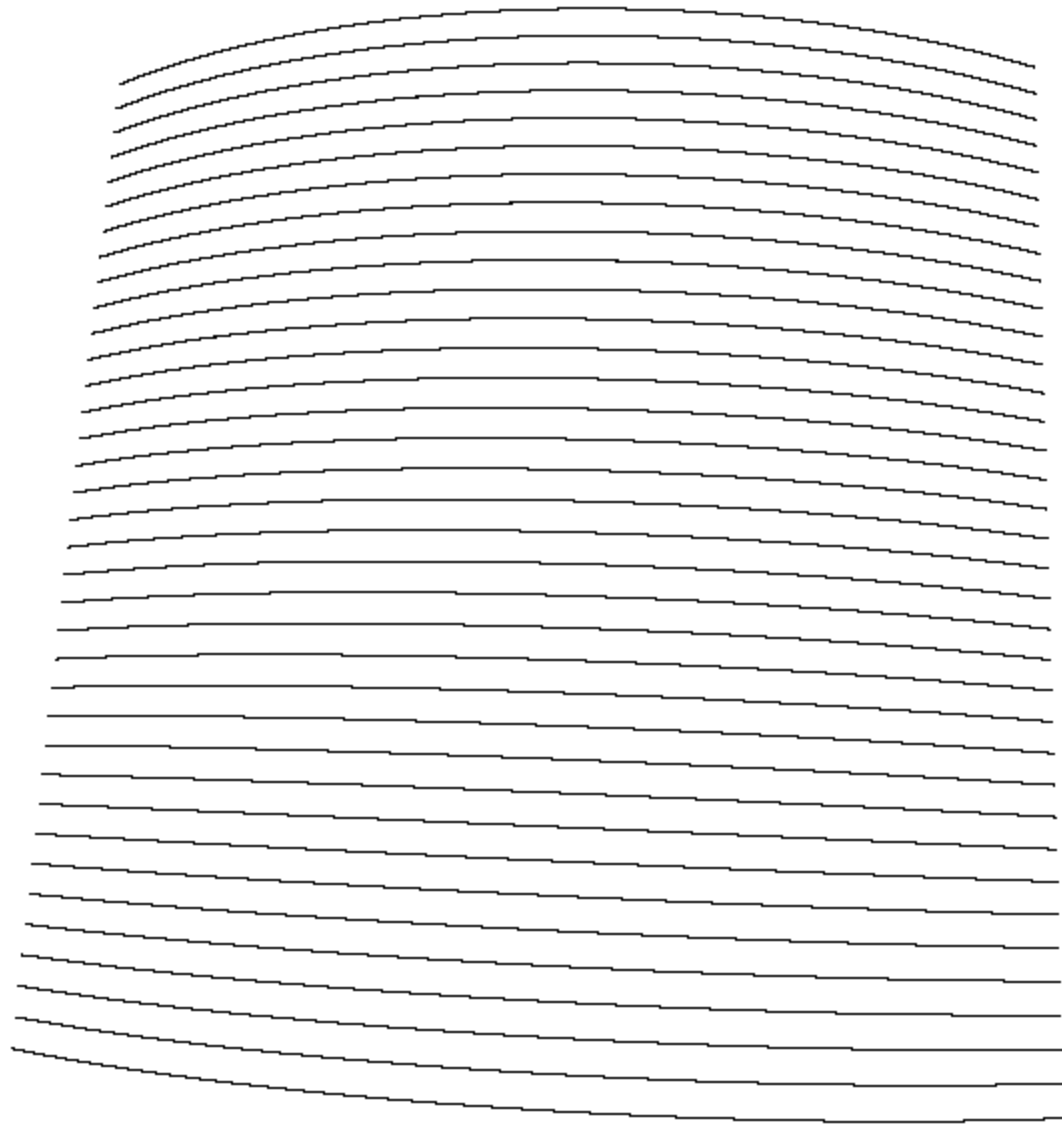


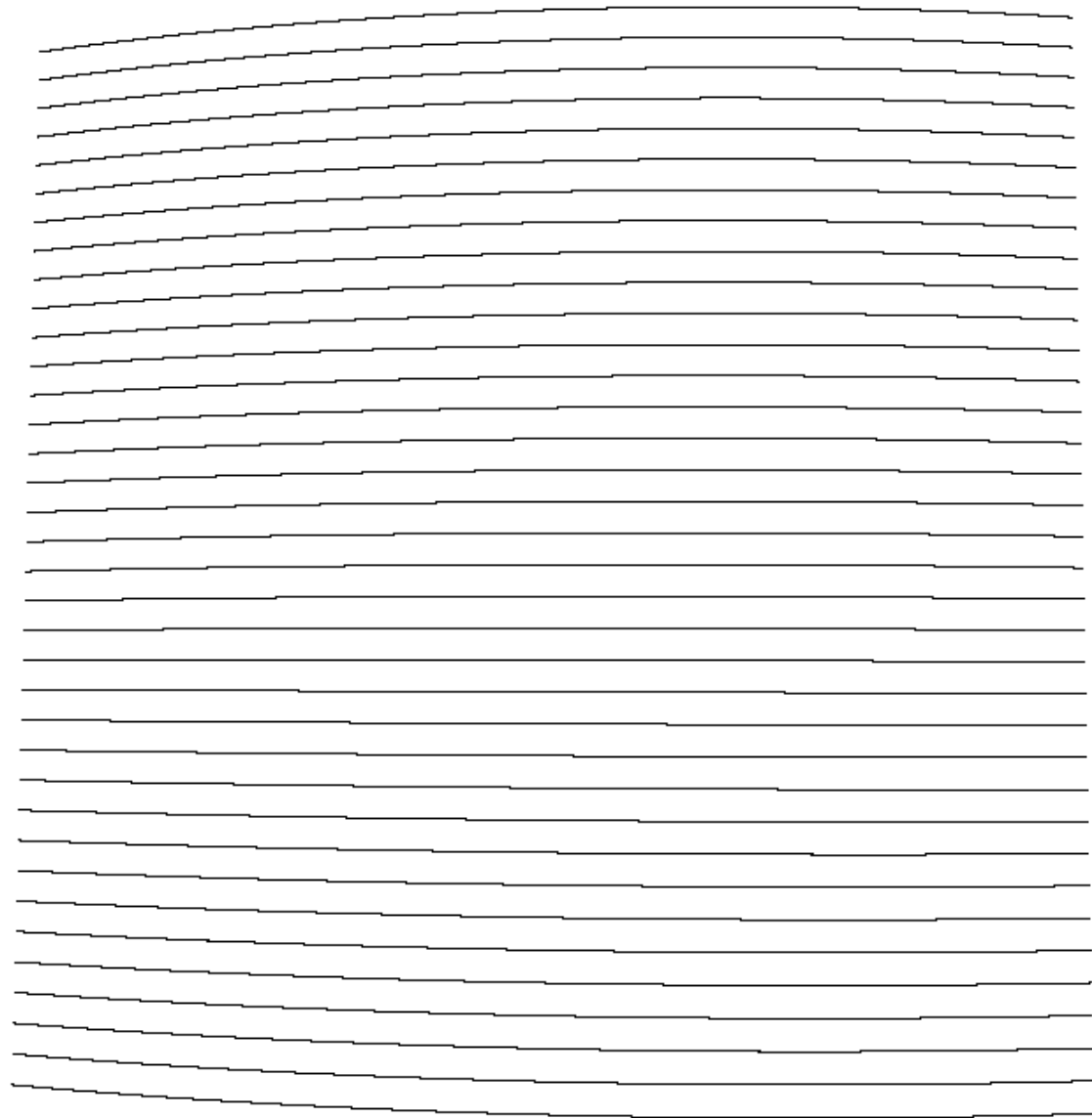


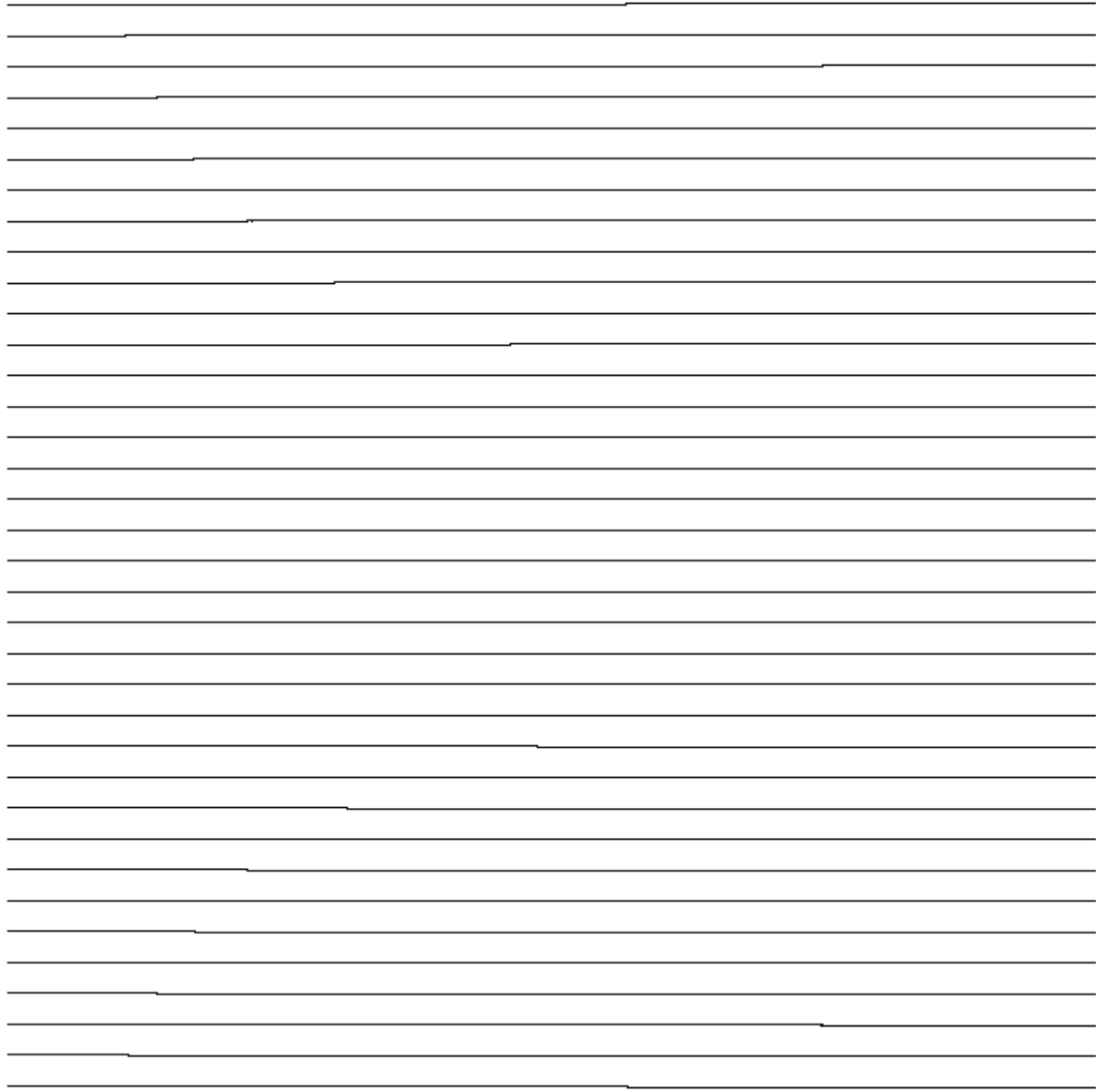




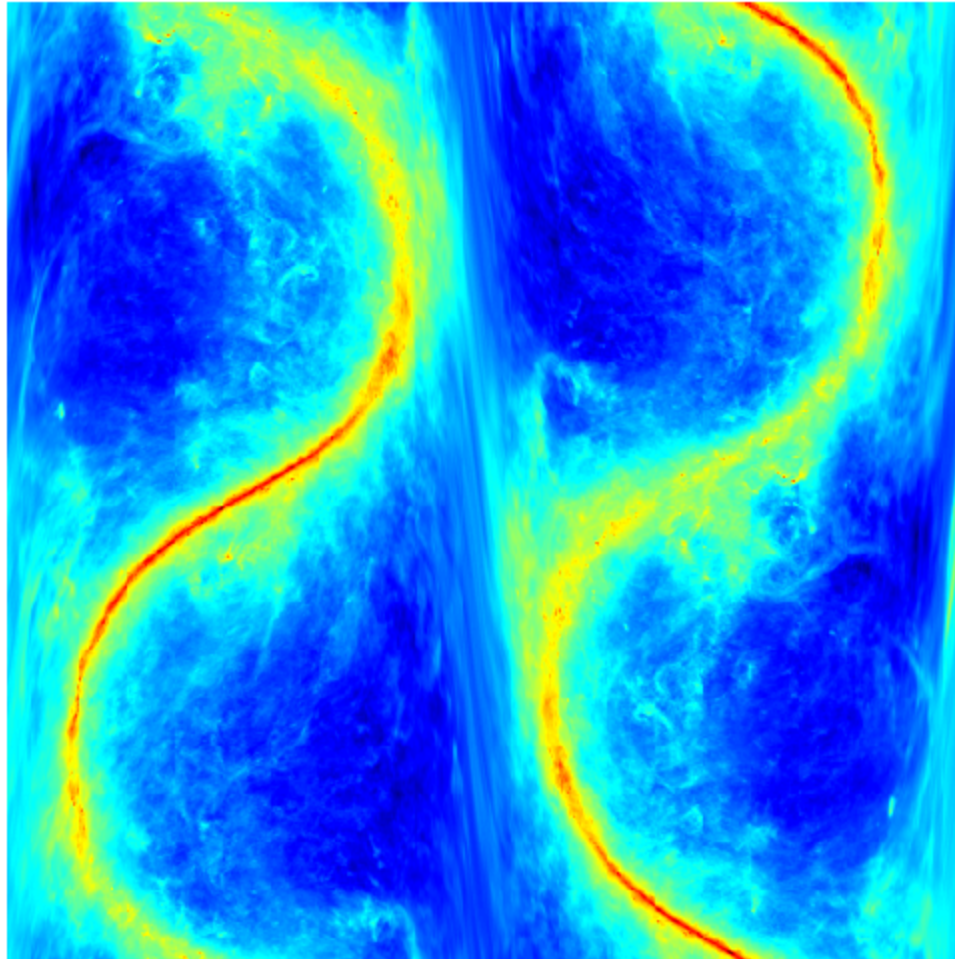






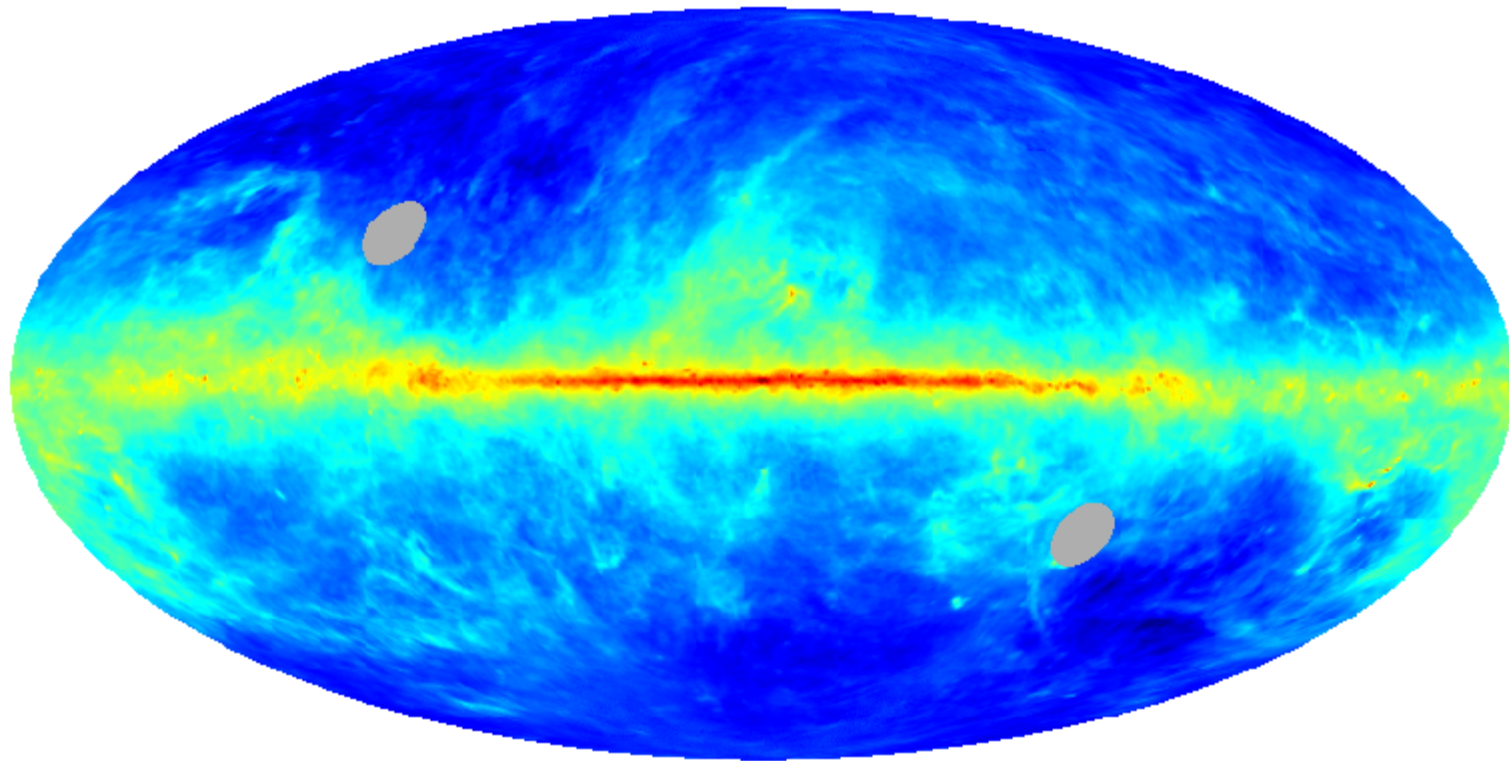


Main beam convolution



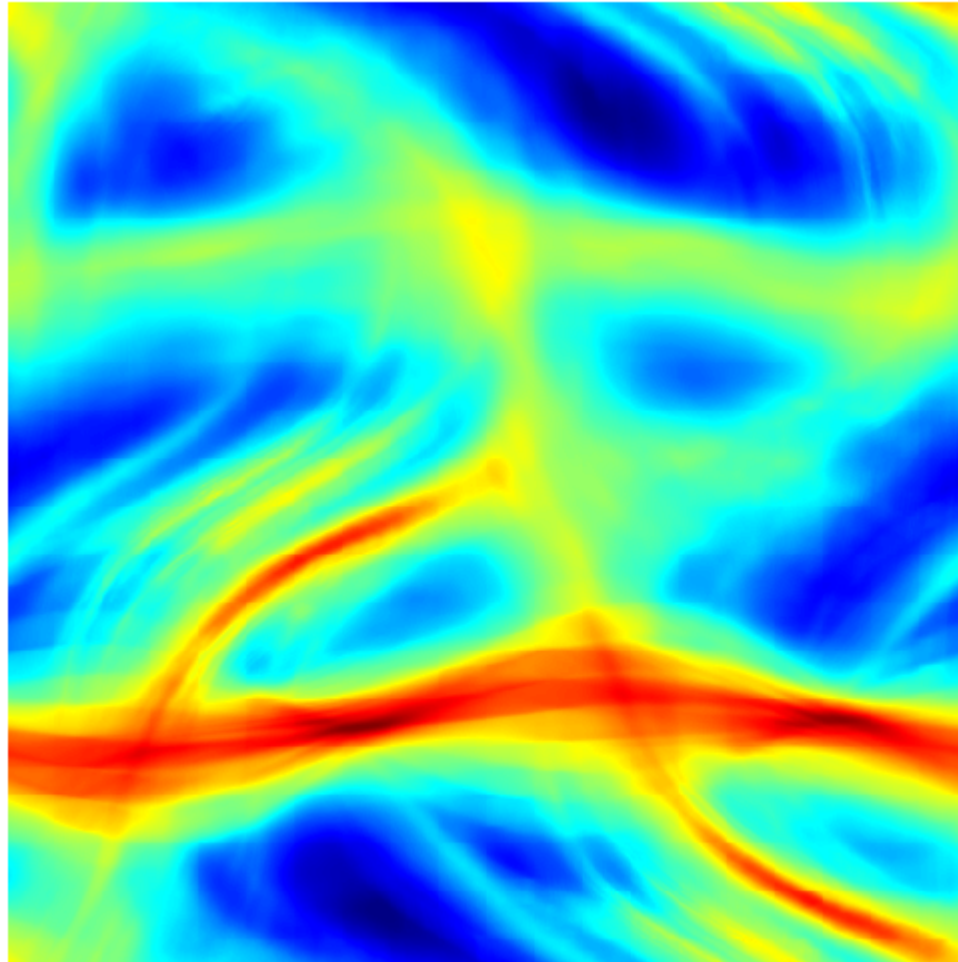
-41.6 dB  0 dB

Main beam convolution



-41 dB  0 dB

Far-side lobe convolution

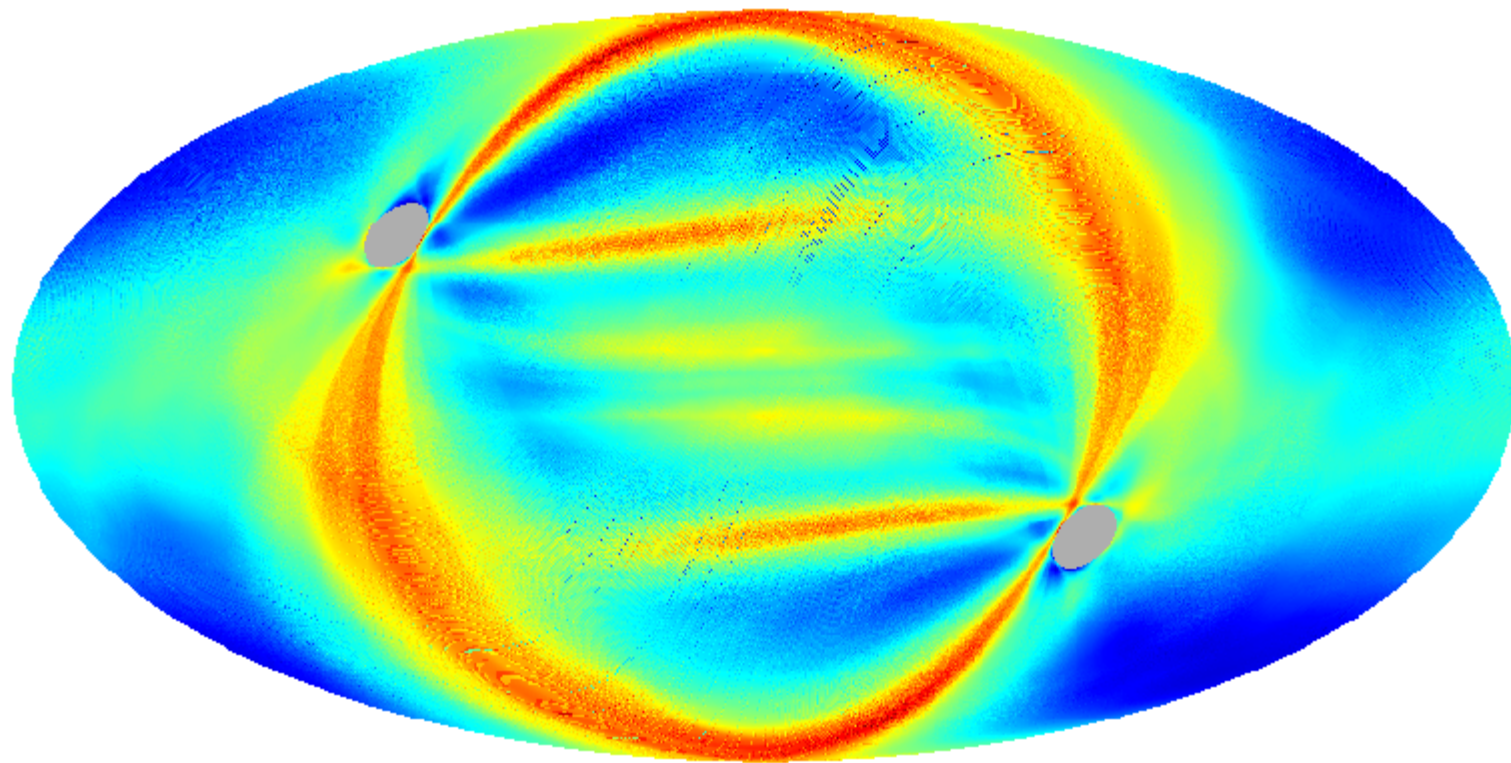


-50 dB



-34 dB

Far-side lobe convolution



-50 dB



-36 dB

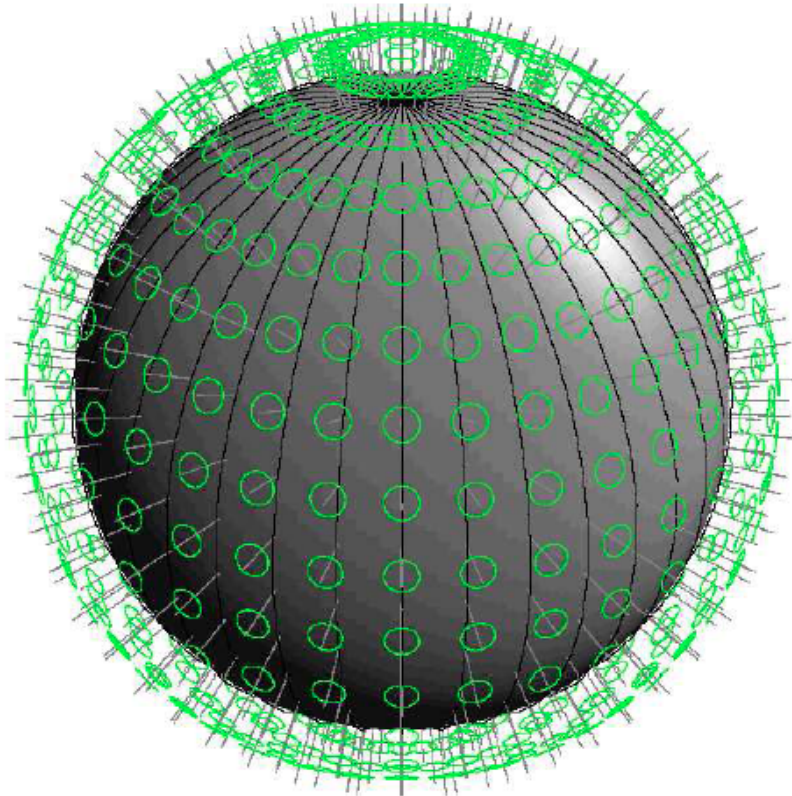
Polarization and higher spin just worksTM

- Everything generalizes to polarized skies and beams (and arbitrary tensor fields on the sphere).

A. Challinor, P. Fosalba, M. Ashdown,
B. D. Wandelt, K. Gorski 2000 astro-ph/0008228

Summary: SO(3) and the 3-torus

BW, astro-ph/0012416



$$T^S(\Phi_2, \Theta, \Phi_1) = \int d\Omega_\gamma \left[\hat{D}(\Phi_2, \Theta, \Phi_1) b \right](\gamma)^* s(\gamma)$$

- For operations involving SO(3) represent in terms of mode functions on the 3-torus
- This gives
 - A fast general convolution algorithm for arbitrary functions (Wandelt & Gorski 2000, arXiv:astro-ph/0008227)
 - An exact fast transform and sampling theorem on the sphere for spin-s spherical harmonics (Huffenberger & BW 2010 ; improved by a factor of 2 by J. McEwen & Wiaux 2011)

Other convolution fun

- GPU accelerated convolution for compact kernels
- Hybrid GPU+CPU algorithm for non-compact convolution kernels
- Compressed convolution

Standard spherical convolution algorithm

$$s(\mathbf{n}_1) = \int_{S^2} K(\mathbf{n}_1, \mathbf{n}_2) r(\mathbf{n}_2) d^2 \mathbf{n}_2 \quad \text{Kernel convolution}$$

For *radial* kernels $K(\mathbf{p}, \mathbf{q}) = K(p \cdot q) \quad p \cdot q \equiv \mathbf{n}_p \cdot \mathbf{n}_q$

$$K(p \cdot q) = \sum_{\ell} \frac{2\ell + 1}{4\pi} K_{\ell} P_{\ell}(p \cdot q) \quad \text{Legendre decomposition}$$

$$K_{\ell} = 2\pi \int_{-1}^1 K(z) P_{\ell}(z) dz$$

$$s_{\ell m} = K_{\ell} r_{\ell m}$$

Scales as $O(L^3)$, dominated by spherical harmonic transforms

Why move beyond FSHT convolution for radial kernels?

- Spherical Harmonic Transforms are hard to parallelize
- For high resolution problems ($L_{\max} > 1024$) the recursions for the spherical harmonics $Y_{lm}(n)$ need to be computed in extended double precision to avoid underflows.
- Too general for many problems – does not exploit kernel compactness

Hybrid convolution algorithm idea: avoid spherical harmonic transform

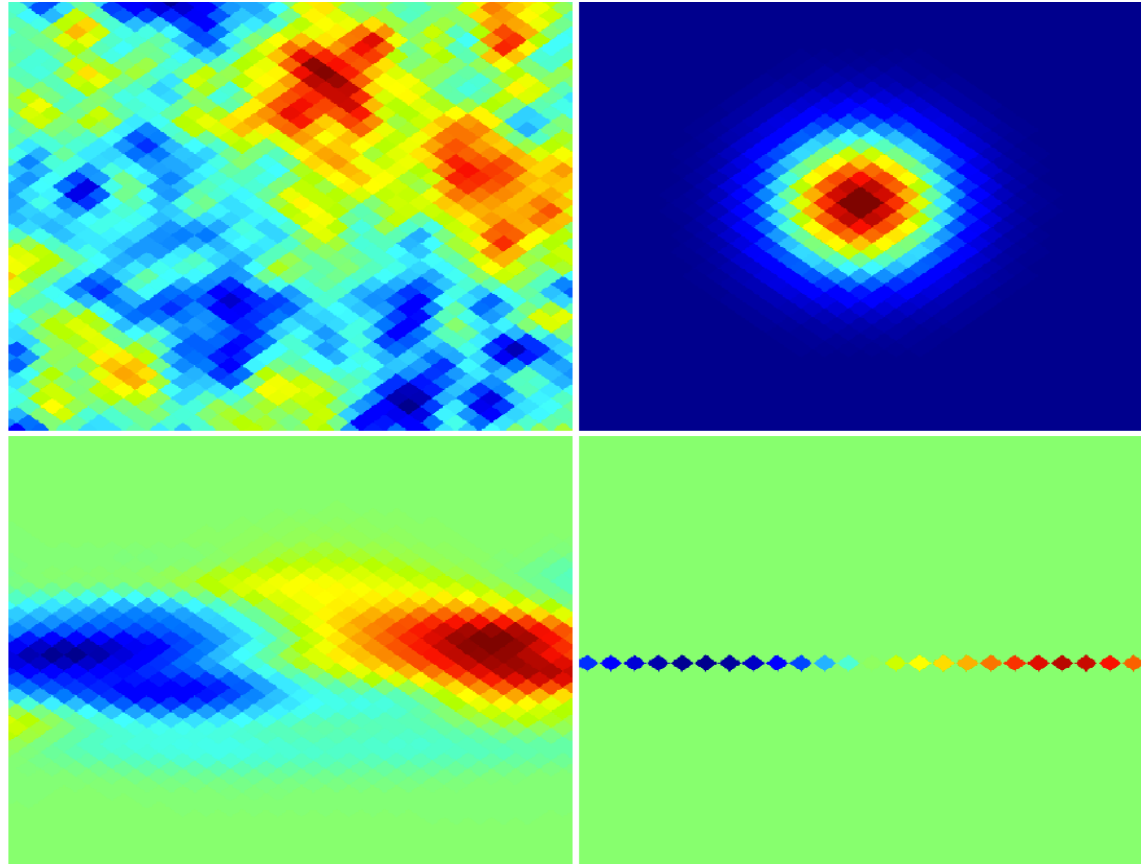
Generate convolved map ring by ring using batch 1-D FFTs (CUDAFFT)

The figure shows the generation of one output ring.

Hybrid method allows exploiting kernel compactness



Scaling to convolve entire map is $O(\text{kernelwidth } npix \log(npix))$



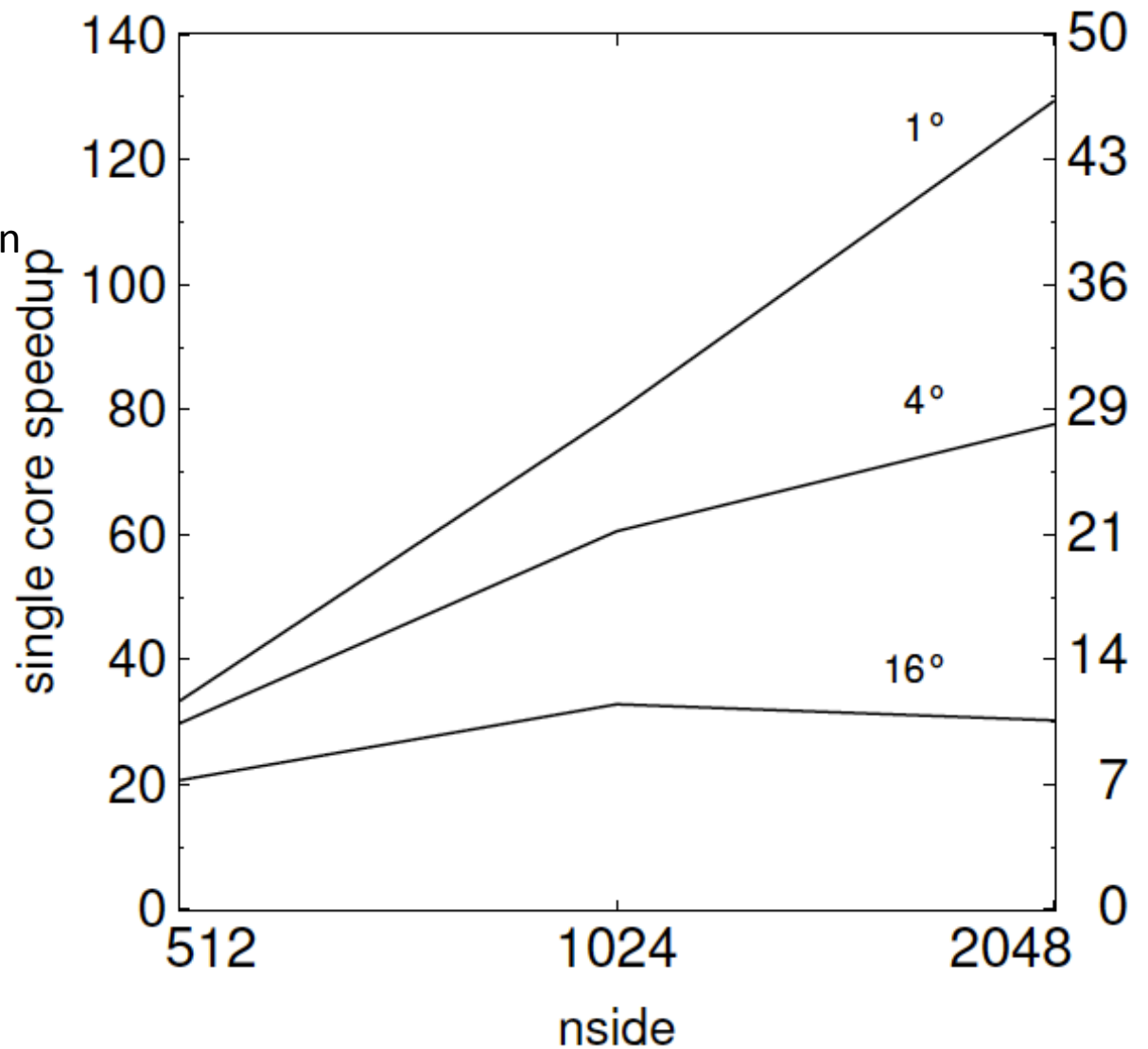
ARKCOS: Speed-up compared to SHT convolution

Left axis:
HEALPix SHT implementation

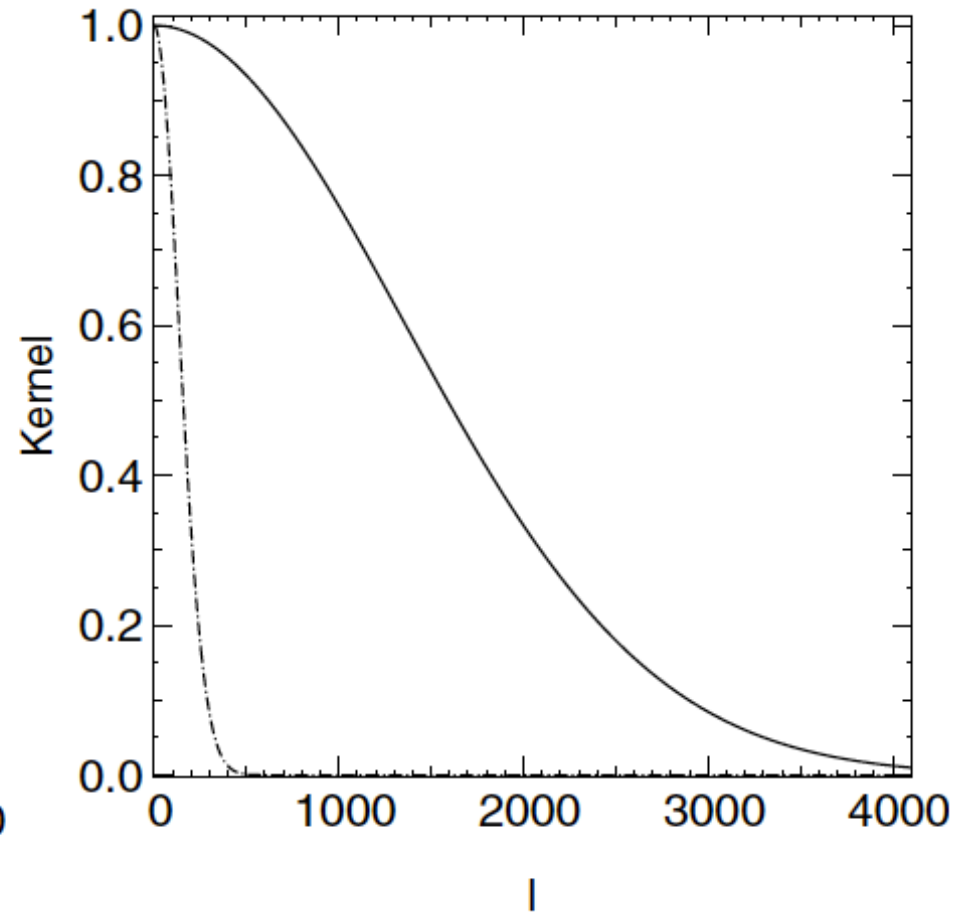
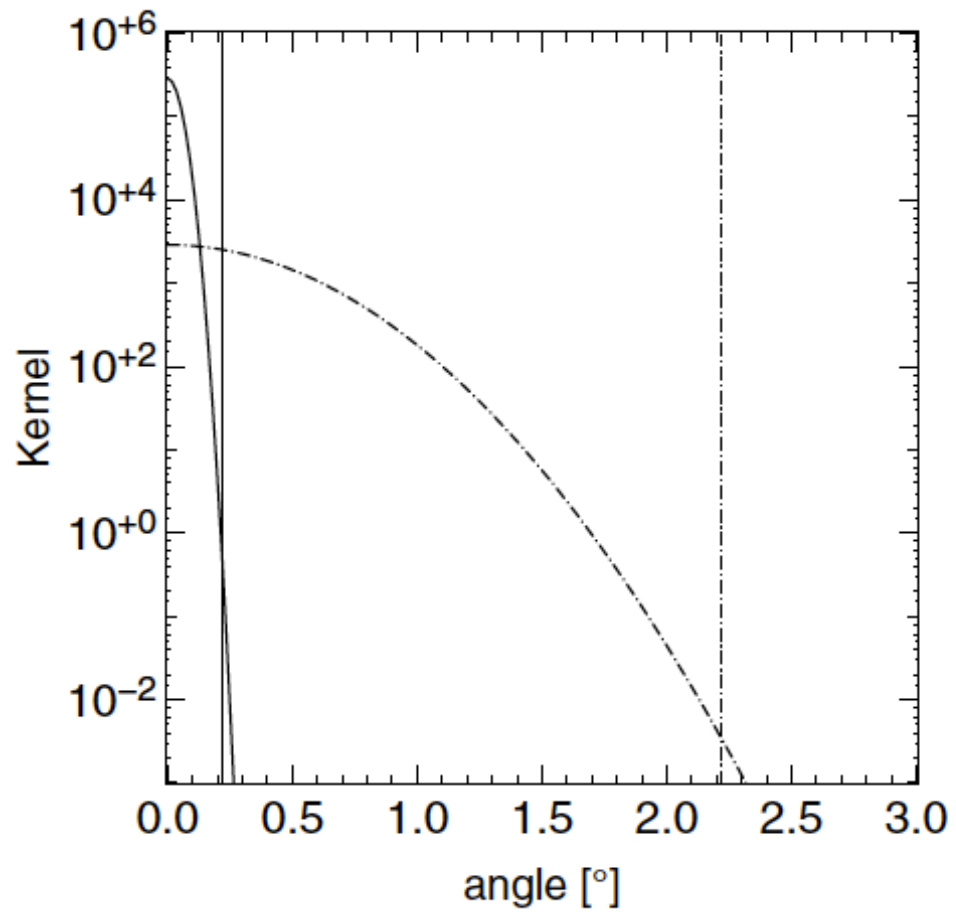
Right axis:
libshft implementation
(highly optimized)

Arkcos:
Elsner & Wandelt 2011,
Astr. & Astrophys. 532, A 35
(arXiv:1104.0672)

**Example at nside 2048,
5 x 10⁷ pixels**

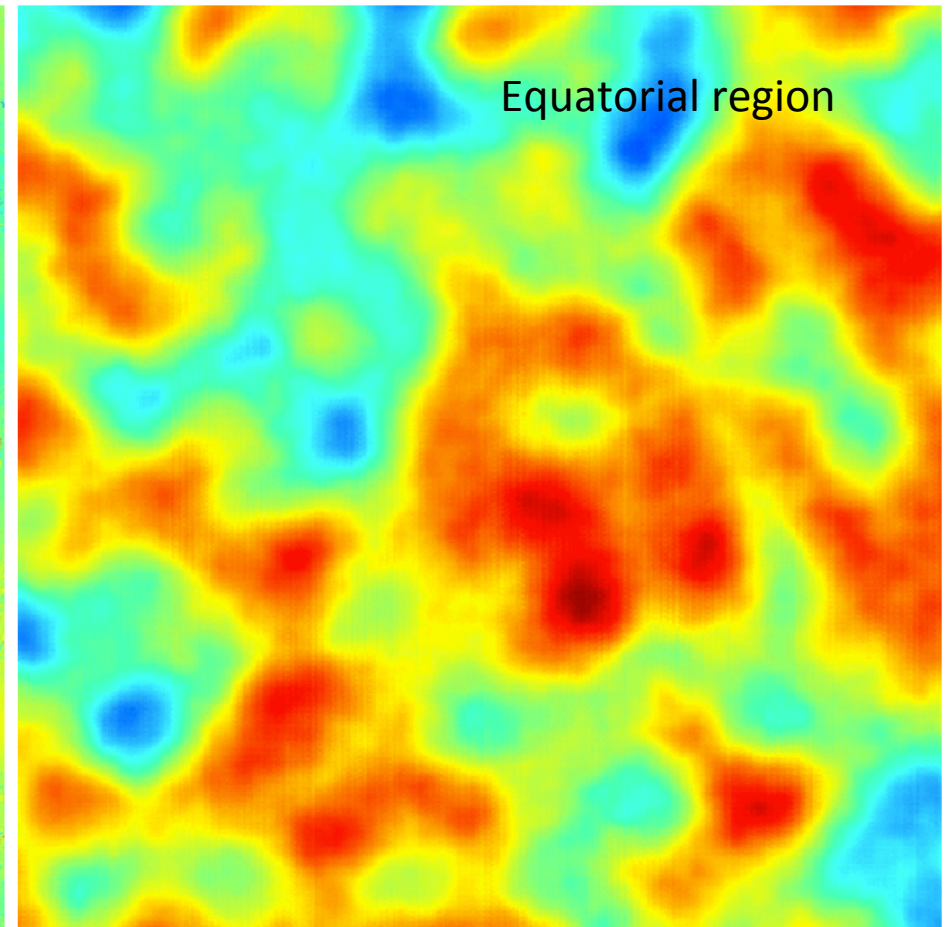
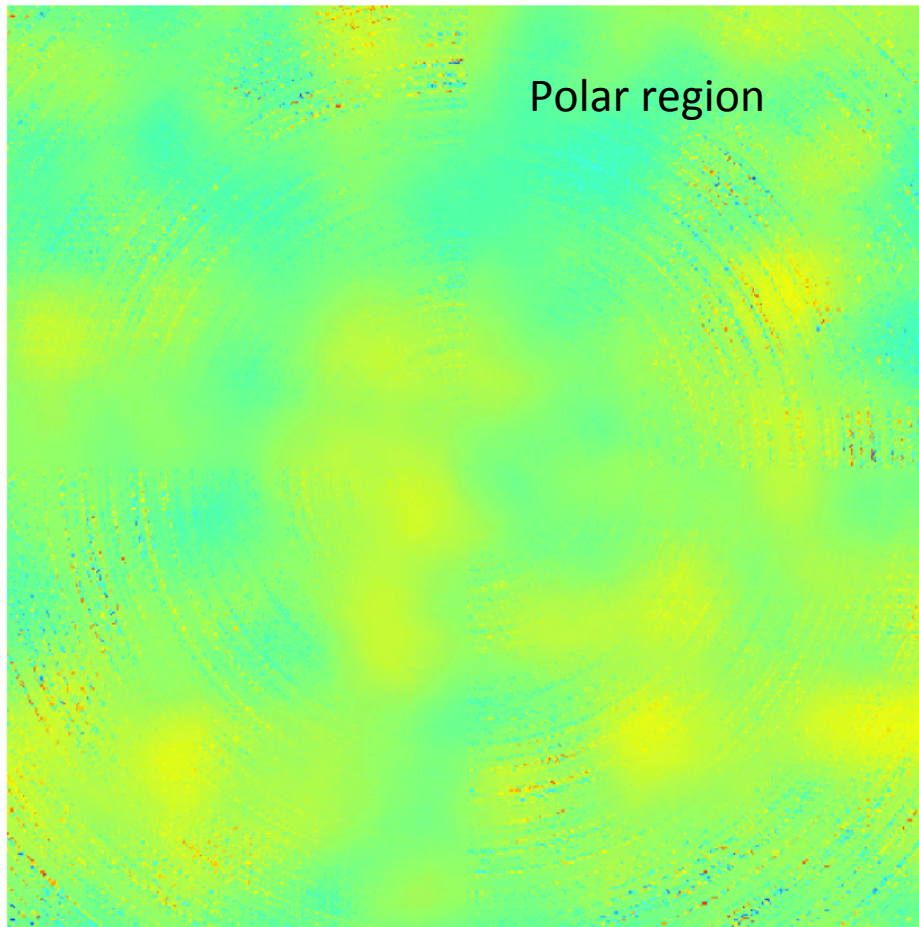


Test kernels



Accuracy: map diagnostic

RMS accuracy better than 0.0001

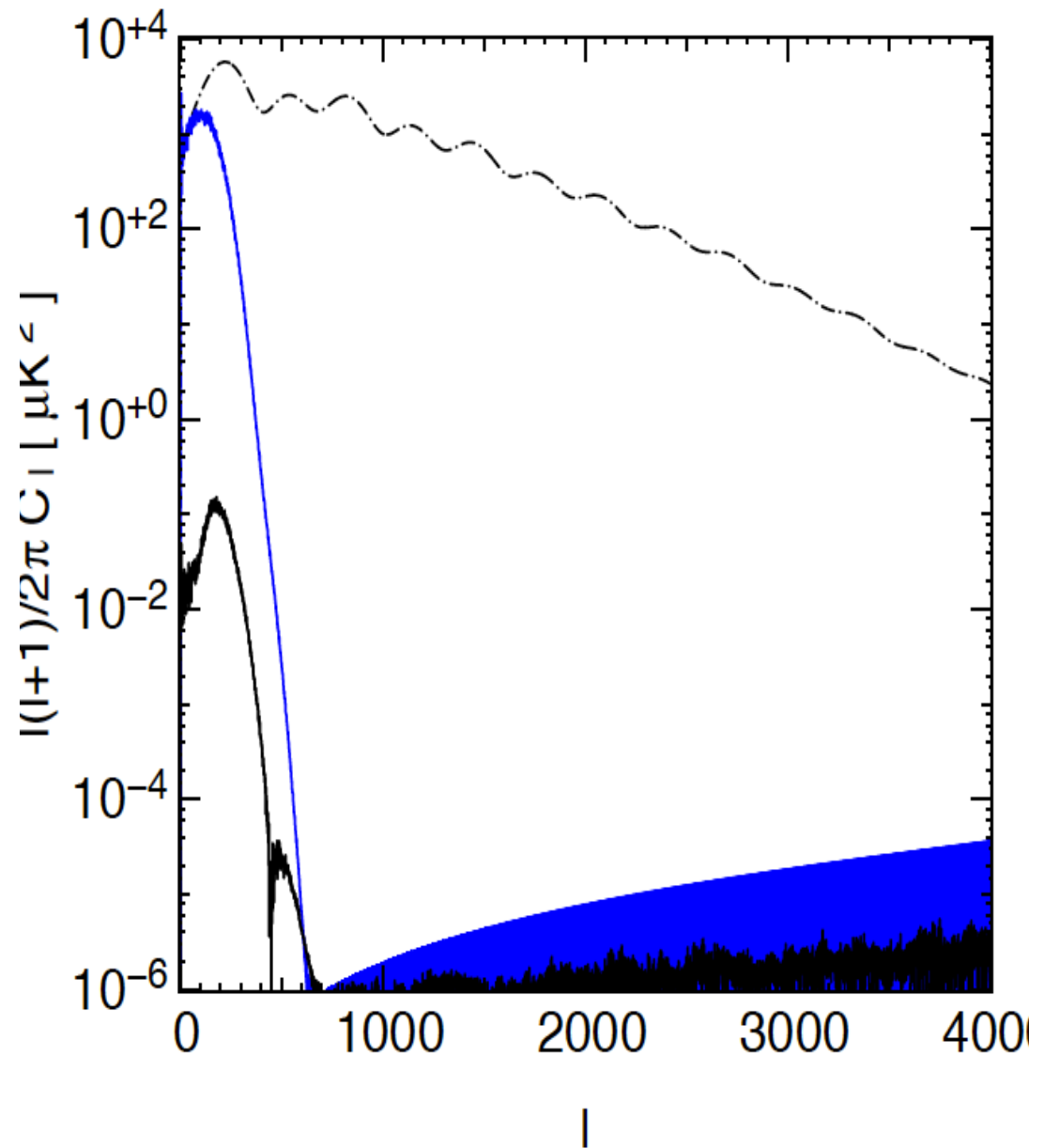


Accuracy: Power spectrum diagnostic

Smoothing with a Gaussian kernel
FWHM 1 degree

Smoothed map

Difference spectrum



GPU optimization

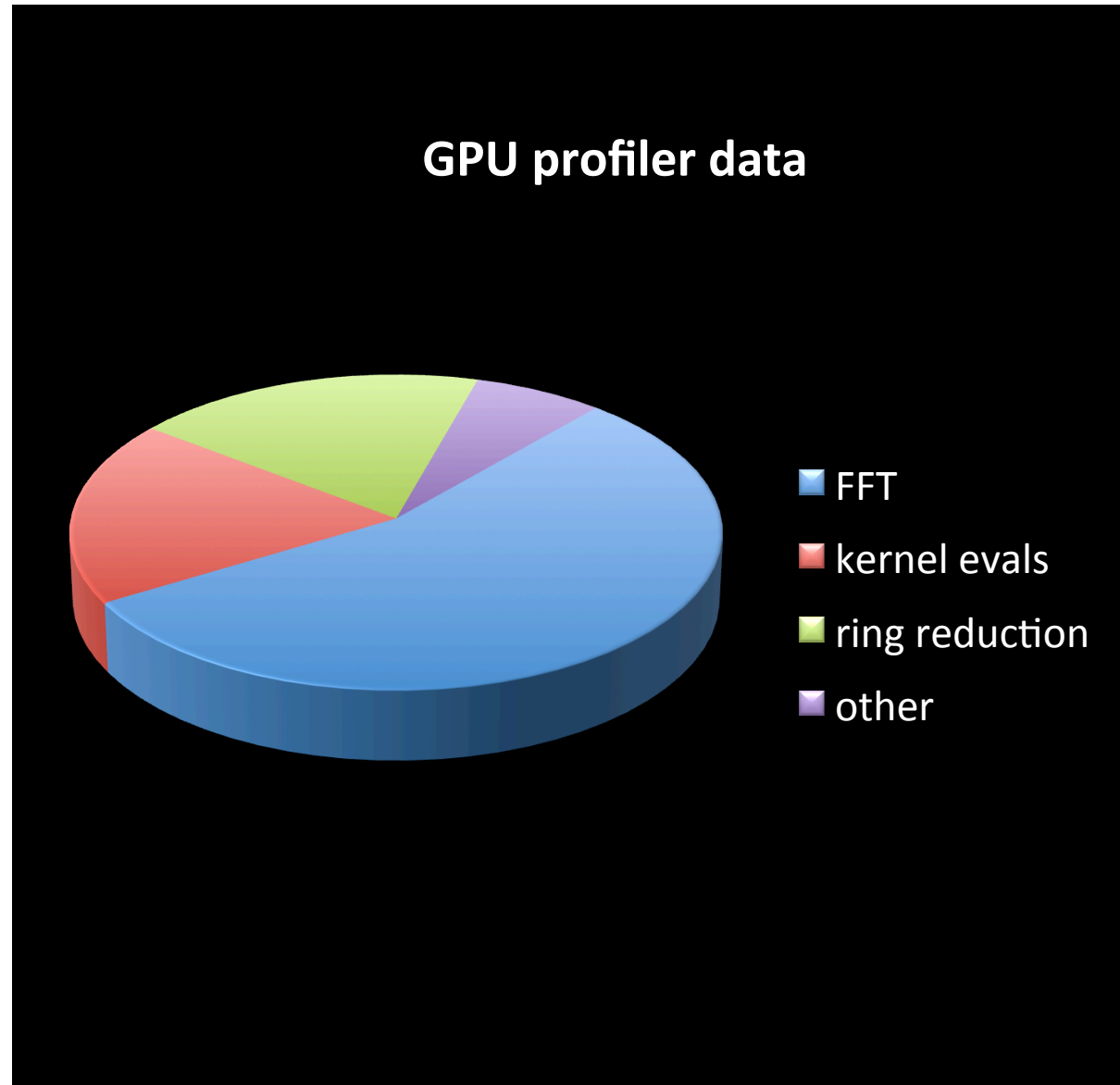
Minimize memory latency
– reach over 80% of theoretical peak memory bandwidth (144GB/s out of 170 GB/s)

Exploit high level of data parallelism

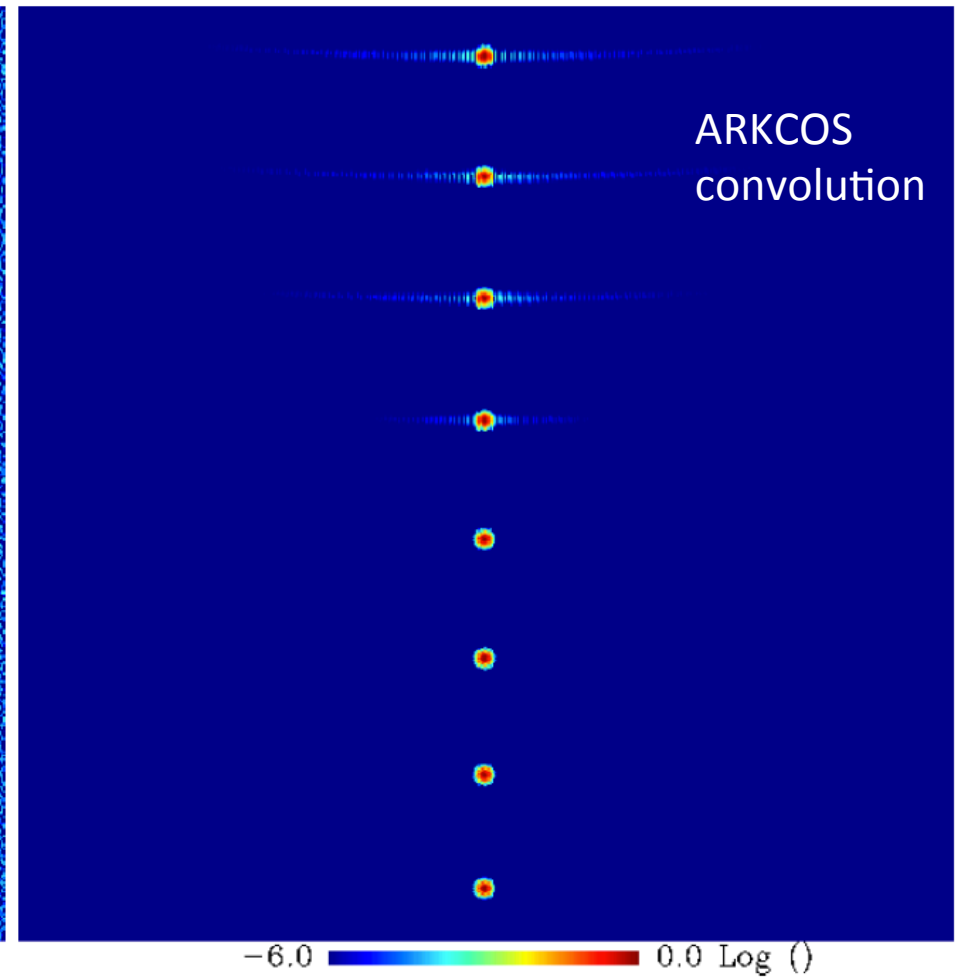
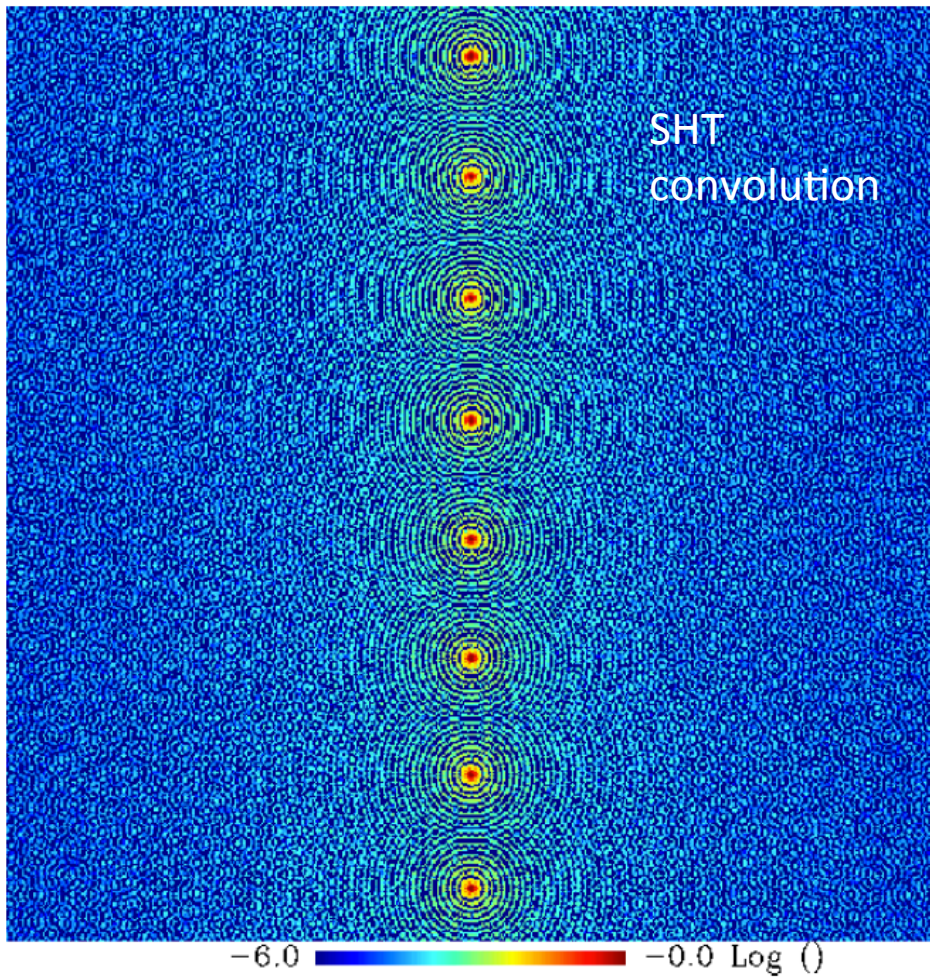
Instruction level parallelism

Use optimized library for batch FFTs (CUFFT)

Use single precision floats whenever possible



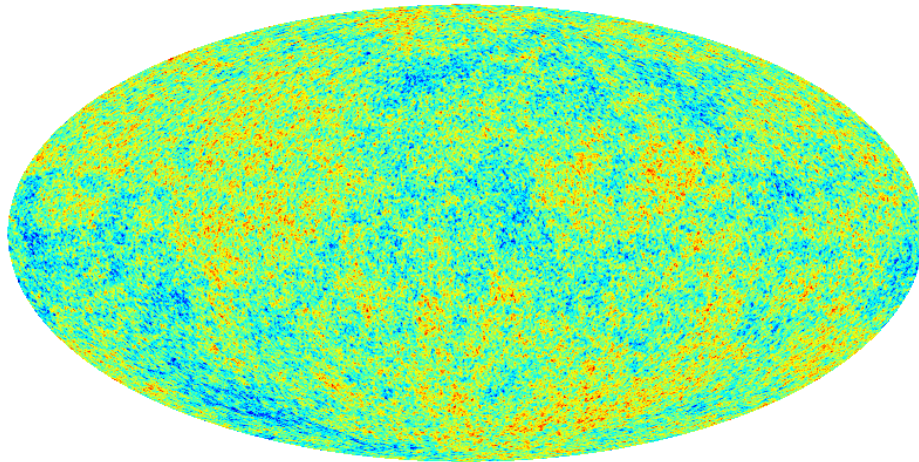
Side effect: suppress ringing artifacts



Generalization to non-compact kernels

- Split kernel into two parts:
 - one that is compact in real space and
 - one that is compact spherical harmonic space
- Solve optimization problem to choose bandlimit and kernel footprint for the split to maximize predicted speed-up while respecting error bound
- Then perform convolution in parallel
 - SHT on CPU
 - ARKCOS on GPU

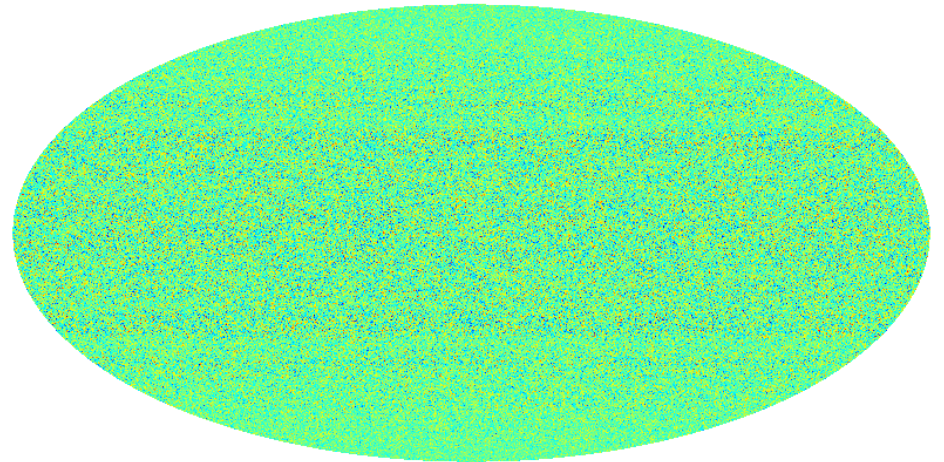
Kernel splitting results: 15x speed up



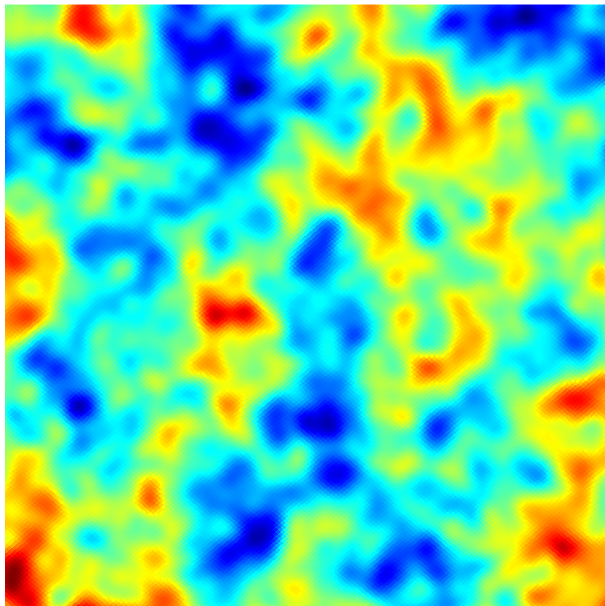
Full



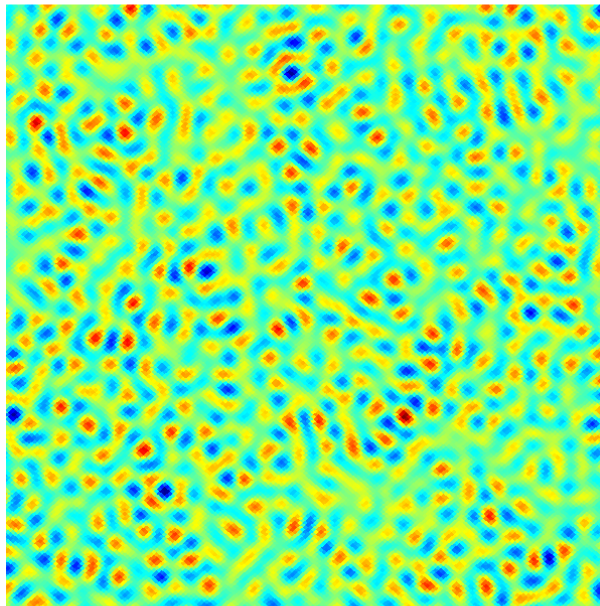
1-space difference



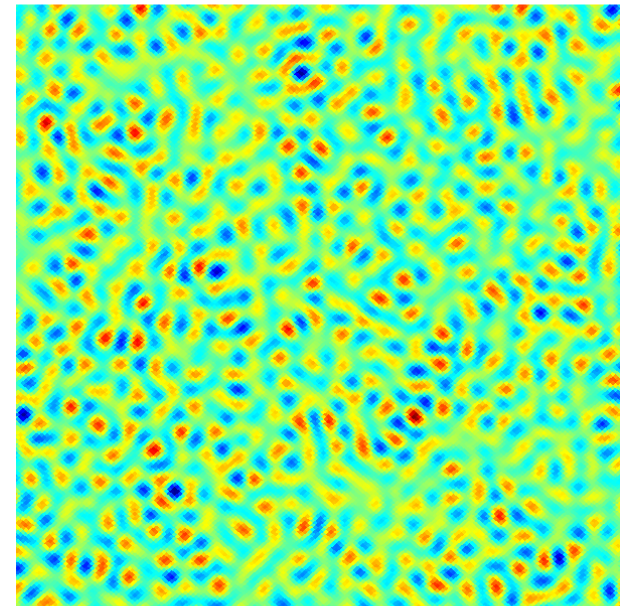
ARKCoS



-0.00026 0.00023 K



-2.1e-06 2.1e-05 K



-2.1e-06 2.1e-05 K

Compressed convolution reduces redundancy for large filter banks

- Problems with large filter banks:
 - "Continuous" wavelet expansion
 - Searching for many different "objects" (bubble collisions/textures in CMB or gravitational wave templates etc.) of unknown size
 - Simulations of CMB observations from 10^2 - 10^5 different detectors

Compressed Convolution

- For an arbitrary set of kernels $s_i^{(n)} = \sum_j K_{i,j}^{(n)} d_j$
- One can expand the kernels in an small $O(k)$ optimal basis to minimize the convolution error of all the outputs $K_{i,j} = \sum_k \lambda^k \hat{K}(\phi^k)_{i,j}$
- Convolve with the kernel basis set and to obtain a compressed convolution output
- To get each output convolution decompress as needed in $O(k)$ operations per output.

$$s_i^{(n)} = \sum_k \lambda^{(n),k} s_i^k$$

Constructing the basis kernels

- Minimize

$$\begin{aligned}\sigma^2 &= \left\langle \sum_{(n)} \sum_{i, i'} s_i^{(n)} N_{ii'}^{(n)-1} s_{i'}^{(n)} \right\rangle \\ &= \sum_{n, i, i'} N_{ii'}^{(n)-1} (R_{i'} k^{(n)}) C (R_i k^{(n)})^\dagger\end{aligned}$$

for a fixed number k of basis kernels. By Schur's theorem they are the first k eigenvectors of

$$M_{nm} = \sum_{i, i'} \left[\left(N^{(n)-\frac{1}{2}} \right)^\dagger N^{(m)-\frac{1}{2}} \right]_{ii'} \left(R_{i'} k^{(m)} \right) C \left(R_i k^{(n)} \right)^\dagger$$

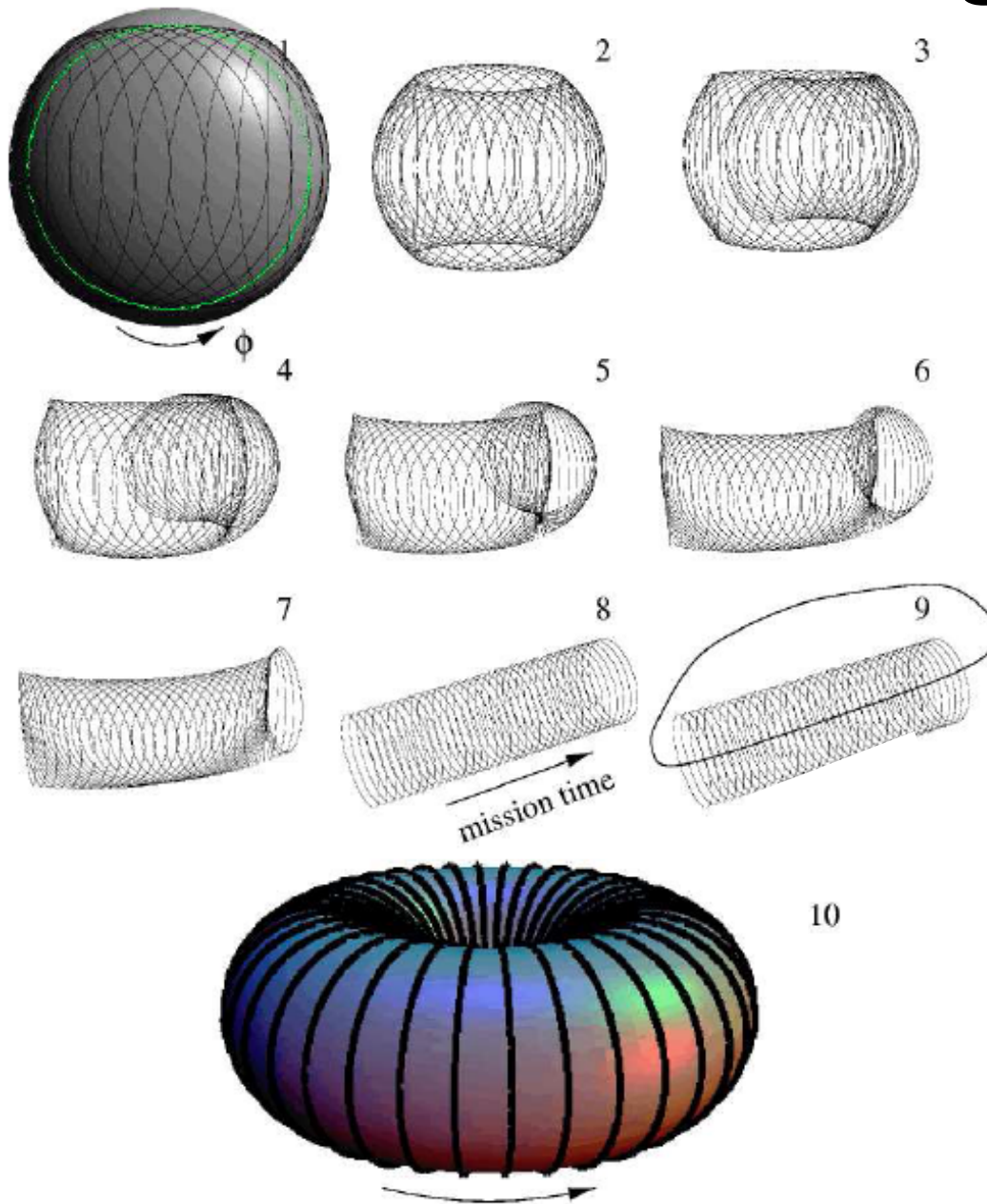
Torus representation of the sphere

- What are the best basis functions to represent functions on the sphere?
- Standard answer:

Isotropy \Rightarrow Spherical Harmonics

But in the absence of fast, high-res non-Abelian transform on $SO(3)$ (and maybe even more generally) the answer is not as clear cut.

Tools: the ring torus



- Can represent all or part of the sphere in terms of a torus double-cover.
- Then use the obvious Fourier basis.

Fisher matrix

- For an isotropic signal on the sphere, the likelihood for the power spectrum C_l is

$$\mathcal{L}(C_\ell|d) = \frac{1}{\sqrt{|2\pi(\mathbf{S}(C_\ell) + \mathbf{N})|}} \times \exp \left[-\frac{1}{2} d^\dagger (\mathbf{S}(C_\ell) + \mathbf{N})^{-1} d \right]$$

- The Fisher matrix is very useful for the Cramer-Rao bound ML estimation, etc..

$$F_{\ell_1 \ell_2} = - \left\langle \frac{\partial^2 \ln \mathcal{L}}{\partial C_{\ell_1} \partial C_{\ell_2}} \right\rangle = \frac{1}{2} \text{tr} [\mathbf{C}^{-1} \mathbf{P}^{\ell_1} \mathbf{C}^{-1} \mathbf{P}^{\ell_2}]$$

- But cannot compute it! $O(l_{max}^6)$ for bandlimit l_{max}

Tegmark arXiv:astro-ph/9611174

Signal correlations on the ring torus

$$\begin{aligned} \mathcal{T}_{mm' MM'} &= \langle T_{mm'} T_{MM'} \rangle \\ &= \boxed{\delta_{mM}} \sum_l C_l d_{mm'}^l(\theta_E) X_{lm'} d_{MM'}^l(\theta_E) X_{lM'} \end{aligned}$$

Signal correlation becomes block diagonal!

Fisher matrix on the ring torus

- Go via ring torus basis – amazing property

$$\begin{aligned} \left(\frac{\partial \mathbf{C}_r}{\partial C_\ell} \right)_{pp'} &= \left(\frac{\partial \mathbf{S}_r}{\partial C_\ell} \right)_{pp'} \\ &= N^2 d_{rp}^\ell X_{\ell p} d_{rp'}^\ell X_{\ell p'}^* \\ &= q_{rp}^\ell q_{rp'}^{\ell*}, \end{aligned}$$

the derivative in the torus basis is **rank 1**, as opposed to rank l in the spherical harmonic basis. So the torus basis gives a more compact representation for an isotropic signal than spherical harmonics!

Franz Elsner, BW
arXiv: 1202.4898
arXiv: 1205.0810

Bayesian power spectrum inference

- For an isotropic signal on the sphere, the likelihood for the power spectrum C_ℓ is

$$\mathcal{L}(C_\ell|d) = \frac{1}{\sqrt{|2\pi(\mathbf{S}(C_\ell) + \mathbf{N})|}} \times \exp \left[-\frac{1}{2} d^\dagger (\mathbf{S}(C_\ell) + \mathbf{N})^{-1} d \right]$$

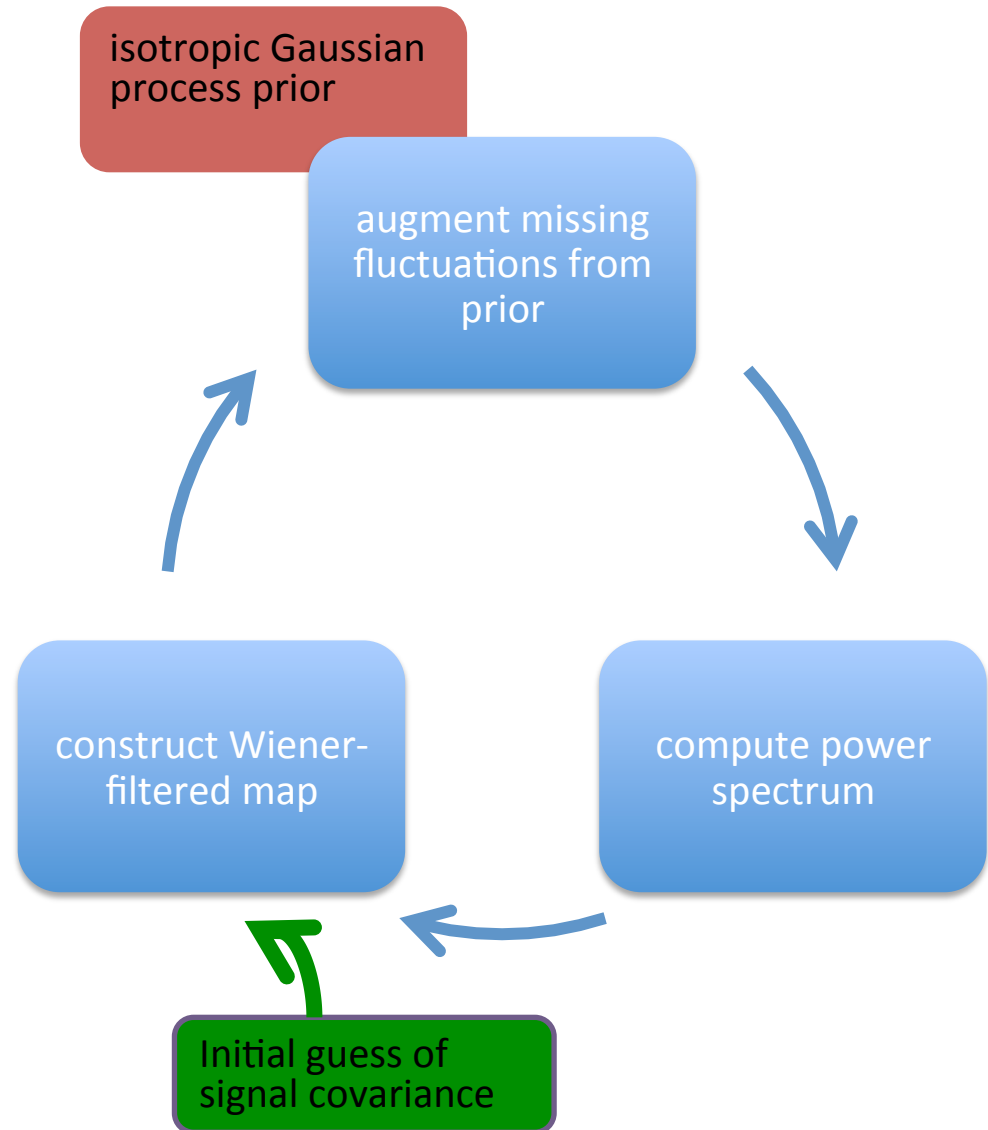
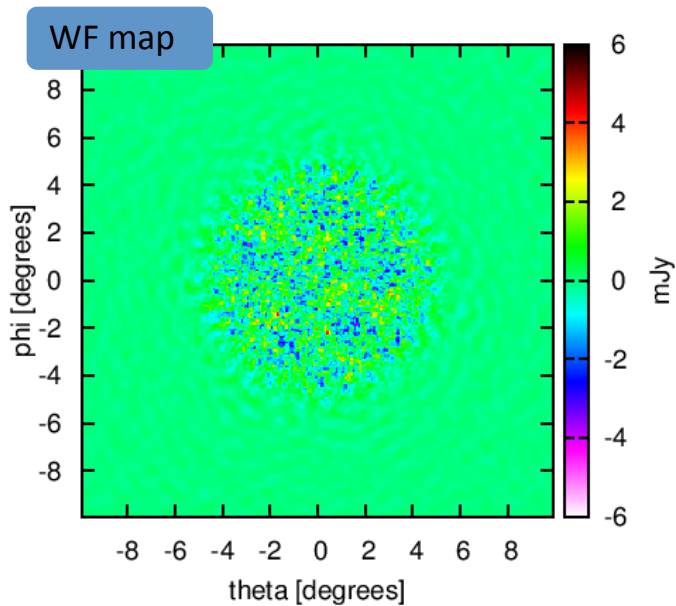
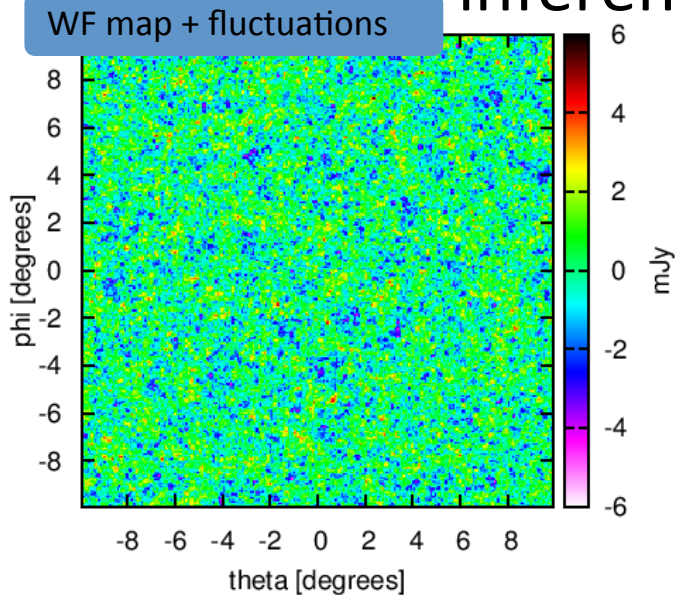
- But cannot compute it! $O(l_{max}^6)$ for bandlimit l_{max} . For Planck, $l_{max}=2500$, so $t_{CPU} = 10^4$ years, for a single evaluation

Gibbs sampling

- Augment the model with the signal map \mathbf{s} – adds $O(10^7)$ parameters
- Gibbs sampling iteratively draws from the conditional densities $P(\mathbf{s} | \mathbf{d}, \mathbf{C}_l)$ and $P(\mathbf{C}_l | \mathbf{s})$ with a acceptance ratio **1**.
- This is possible in $O(l_{\max}^3)$ operations, a speed-up of $\sim 10^9$).
- Used in final versions of WMAP and for low-ell Planck analysis.

Jewell, Levin, and Anderson (2004) and
Wandelt, Larson & Lakshminarayanan (2004)

Gibbs sampling is a both power spectrum inference and non-linear Wiener filter



Fundamental operation: Wiener Filter

$$d = s + n$$

Not sparse in any easily accessible basis

$$(\mathbf{S}^{-1} + \mathbf{N}^{-1}) s_{WF} = \mathbf{N}^{-1} d$$

Sparse in Fourier space

Sparse in pixel space

Usual solution strategies

- Iterative conjugate gradients (optimal for SPD matrices)
- Preconditioner (diagonal in Fourier space, multi-grid)
- Problems:
 - For Planck: ***extremely ill-conditioned***, condition number $>10^8$
 - Preconditioner not universal
 - Stability issues (Jacobi smoother in multi-grid)

Wiener Filtering without preconditioner

- Introduce auxiliary field (*messenger* field) t with covariance \mathbf{T} . Then

$$(\bar{\mathbf{N}}^{-1} + (\mathbf{T})^{-1}) t = \bar{\mathbf{N}}^{-1} d + (\mathbf{T})^{-1} s$$

$$(\mathbf{S}^{-1} + (\mathbf{T})^{-1}) s = (\mathbf{T})^{-1} t,$$

$$\bar{\mathbf{N}} \equiv \mathbf{N} - \mathbf{T}$$

is solved by the Wiener filter.

Can solve each of these equations *exactly*.

Iterate. Easy to show that this converges and is unconditionally stable.

Elsner & Wandelt, arXiv:1210.4931

Wiener Filtering without preconditioner

- Introduce auxiliary field (*messenger* field) t with covariance \mathbf{T} and a parameter $\lambda \geq 1$. Then

$$(\bar{\mathbf{N}}^{-1} + (\lambda \mathbf{T})^{-1}) t = \bar{\mathbf{N}}^{-1} d + (\lambda \mathbf{T})^{-1} s$$

$$(\mathbf{S}^{-1} + (\lambda \mathbf{T})^{-1}) s = (\lambda \mathbf{T})^{-1} t,$$

$$\bar{\mathbf{N}} \equiv \mathbf{N} - \mathbf{T}$$

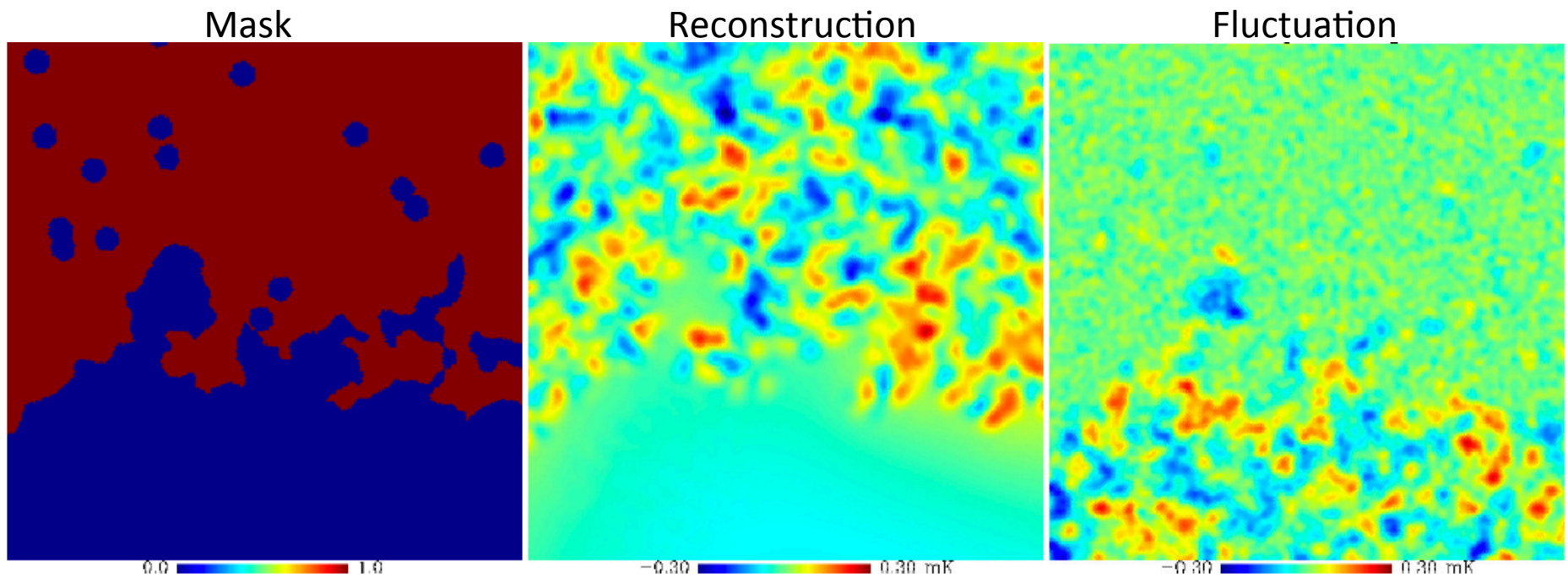
is solved by the Wiener filter for $\lambda=1$.

Can solve each of these equations *exactly*.

Iterate. Easy to show that this converges and is unconditionally stable.

Elsner & Wandelt, arXiv:1210.4931

Optimal reconstruction, filtering and constrained realizations: WMAP temperature data

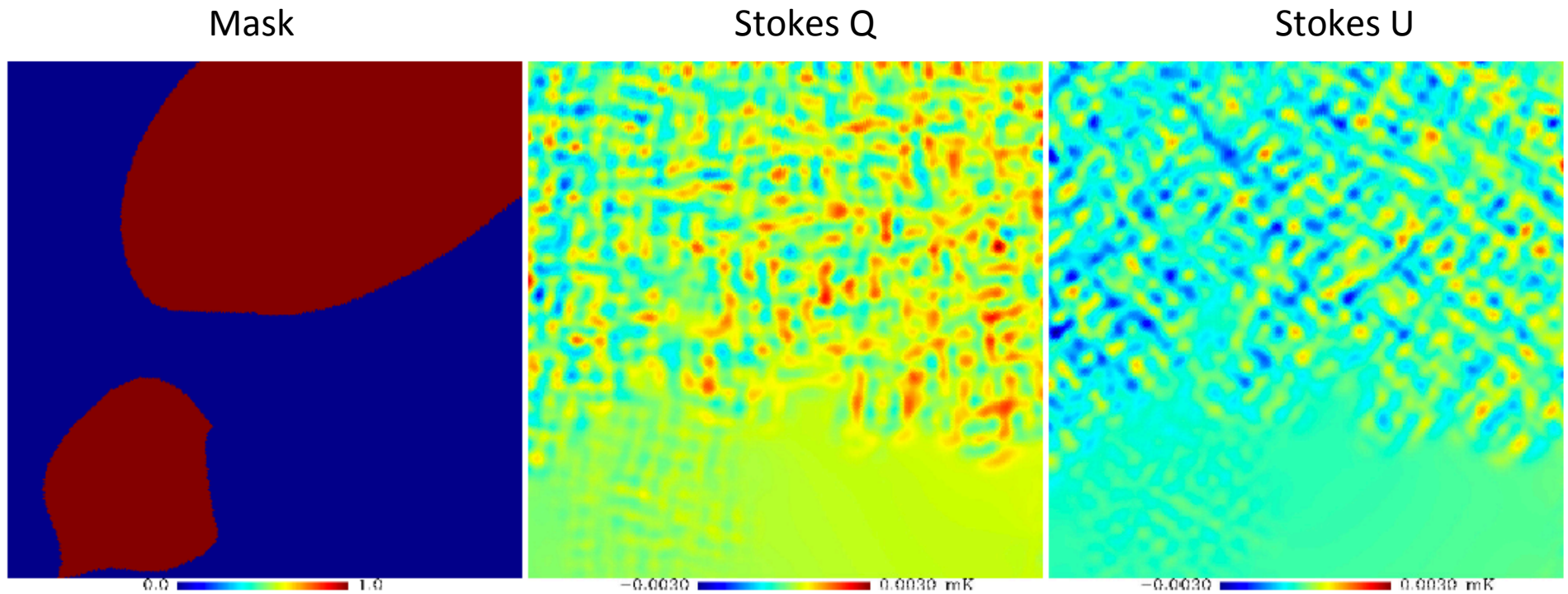


Elsner, Wandelt, arXiv:1210.4931

15/07/14

B. Wandelt

Polarization (WMAP data)

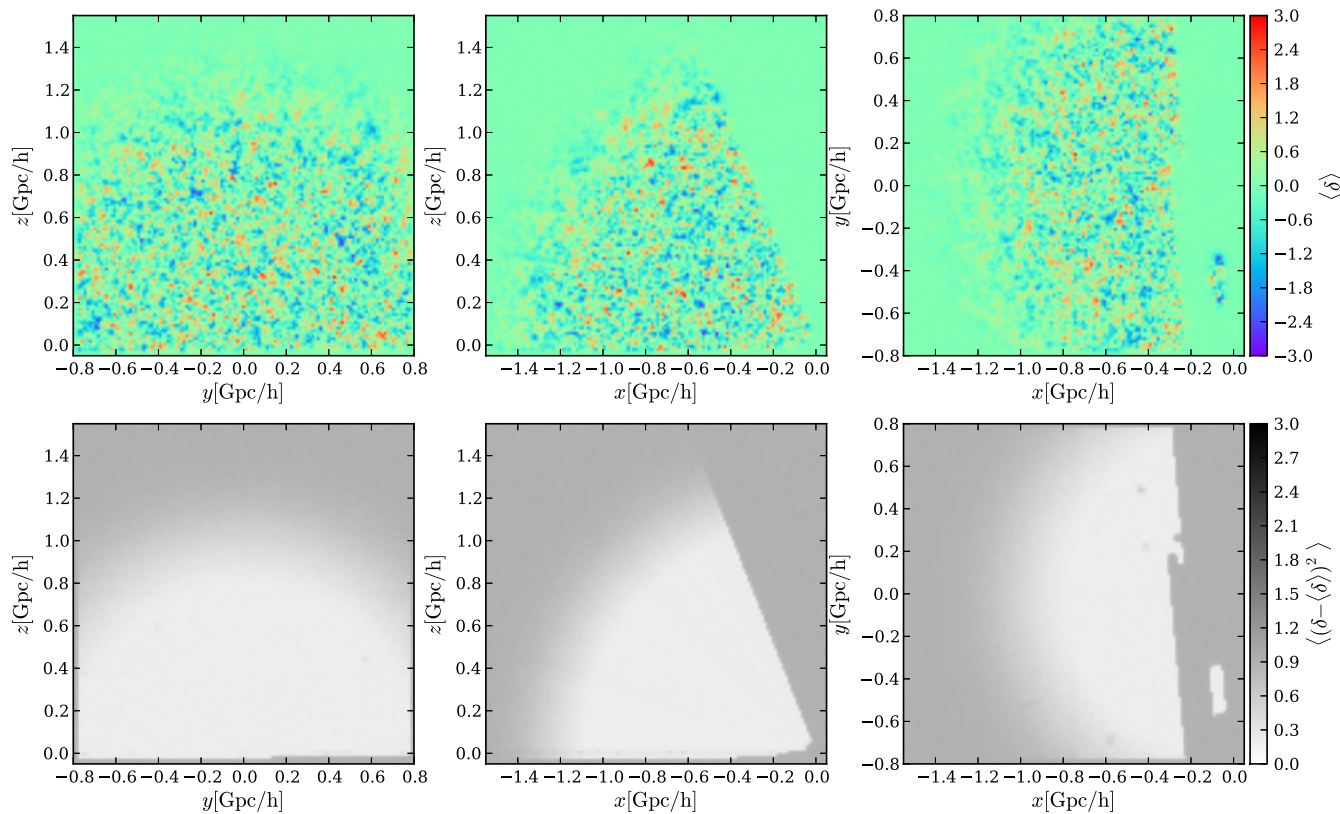


Elsner, Wandelt, arXiv:1210.4931

15/07/14

B. Wandelt

The messenger Wiener filter works even better for 3D LSS signal reconstruction and power spectrum



Jasche, Lavaux, arXiv:1402.1763.

Sampling approaches to GRF model of large scale structure based on previous work with Jasche, Kitaura, Ensslin, Wandelt

Beyond the Gaussian

- Three point correlations encode *shape* information – interest for geophysics?
- For a band-limit of L_{\max} there are $O(L_{\max}^2)$ pixels and $O(L_{\max}^6)$ triangles on the sphere
- For an isotropic field going to spherical harmonics reduces scaling to $O(L_{\max}^5)$.

Bispectrum measurement

Isotropic m-dependence

Theoretical template

$$\hat{f}_{\text{NL}} = \frac{1}{N} \sum_{\ell_i, m_i} \mathcal{G}_{m_1 m_2 m_3}^{\ell_1 \ell_2 \ell_3} b_{\ell_1 \ell_2 \ell_3}^{\text{th}}$$

$$\times \left[C_{\ell_1 m_1, \ell'_1 m'_1}^{-1} a_{\ell'_1 m'_1} C_{\ell_2 m_2, \ell'_2 m'_2}^{-1} a_{\ell'_2 m'_2} C_{\ell_3 m_3, \ell'_3 m'_3}^{-1} a_{\ell'_3 m'_3} - 3 C_{\ell_1 m_1, \ell_2 m_2}^{-1} C_{\ell_3 m_3, \ell'_3 m'_3}^{-1} a_{\ell'_3 m'_3} \right],$$

Variance-reducing
linear term

Weighted data
bispectrum

Meeting the computational challenge

$$\hat{f}_{\text{NL}} = \frac{1}{N} \sum_{\ell_i, m_i} \mathcal{G}_{m_1 m_2 m_3}^{\ell_1 \ell_2 \ell_3} b_{\ell_1 \ell_2 \ell_3}^{\text{th}}$$

Scales as $O(L_{\text{max}}^5)$

$$\times [C_{\ell_1 m_1, \ell'_1 m'_1}^{-1} a_{\ell'_1 m'_1} C_{\ell_2 m_2, \ell'_2 m'_2}^{-1} a_{\ell'_2 m'_2} C_{\ell_3 m_3, \ell'_3 m'_3}^{-1} a_{\ell'_3 m'_3} - 3 C_{\ell_1 m_1, \ell_2 m_2}^{-1} C_{\ell_3 m_3, \ell'_3 m'_3}^{-1} a_{\ell'_3 m'_3}],$$

- Brute force implementation unfeasible for Planck data, $L_{\text{max}} \sim 2000$
- Key idea: KSW – factorization (Komatsu, Spergel, BDW, arXiv:astro-ph/0305189)

$$b_{\ell_1 \ell_2 \ell_3} = \sum_{ijk} X_{\ell_1}^i Y_{\ell_2}^j Z_{\ell_3}^k$$

- Gives $O(L_{\text{max}}^3)$ scaling: $\sim 10^6$ for Planck
- Generalization to more general shapes using sums of separable templates (Fergusson, Liguori, Shellard arXiv: 0912.5516)

Conclusions

- Many operations on spherical data sets are convolutions
- Going to torus representations gives new ways of attacking hard problems and massive speed-ups
- GPU acceleration for radial kernel convolution
- Compressed convolution reduces redundancy for large filter banks